

Self-Selecting Homochiral Quadruple-Stranded Helicates and Control of Supramolecular Chirality

Stephanie A. Boer and David R. Turner*

School of Chemistry, Monash University, Clayton, VIC 3800, Australia.

E-mail: david.turner@monash.edu

Supporting Information

Contents

1. General Experimental Details	2
2. Synthesis.....	5
3. X-Ray Crystallography Details	20
4. Mass Spectrometry	22
5. Powder X-Ray Diffraction	28
6. Thermogravimetric Analysis.....	31
7. Additional Diagrams	34
8. References	41

1. General Experimental Details

Reagents

All starting materials, solvents and reagents were purchased from Sigma-Aldrich, TCI, Merck or Alfa Aesar and used as received.

Nuclear Magnetic Resonance (NMR)

Nuclear magnetic resonance spectra were collected using a Bruker DRX-400 spectrometer in d_6 -DMSO with signals (reported in ppm) referenced against residual solvent peaks. ^{13}C -NMR spectra were collected at 100 MHz and ^1H -NMR spectra were collected at 400 MHz.

Mass Spectrometry

Low resolution mass spectrometry for the dicarboxylic acids was performed using a Micromass Platform Electrospray mass spectrometer in a DMSO/methanol solution as the mobile phase. Low resolution mass spectrometry of the cage complexes was performed using an Agilent 6220 accurate mass LC-TOF system with Agilent 1200 Series HPLC, with an eluent of 0.3 mL/min of acetonitrile. The spectra were fitted with Agilent Multimode Source.

Infrared Spectroscopy

Infrared spectra were obtained using an Agilent Cary 630 diamond attenuated total reflection (ATR) spectrometer. MicroLab software was used to process the data.

Thermogravimetric Analysis

Thermogravimetric analysis (TGA) was conducted using a Mettler TGA/DSC 1 instrument. The temperature was ramped at 5 °C/min from room temperature to 400 °C under a dry N₂ supply of 10.0 mL/min. The data were analysed with the STARe program.

Microanalysis

Microanalyses were performed by either the Campbell Microanalysis Laboratory, Department of Chemistry, University of Otago, Dunedin, New Zealand or the Science Centre, London Metropolitan University, UK.

Circular Dichroism

The circular dichroism spectra of all samples were collected using a Jasco J-815 circular dichroism spectrophotometer. All spectra were collected from 200 – 350 nm in acetonitrile. The cage complexes were run at a concentration of 6 µmol/L and the ligands were run at 60 µmol/L.

Powder X-Ray Diffraction

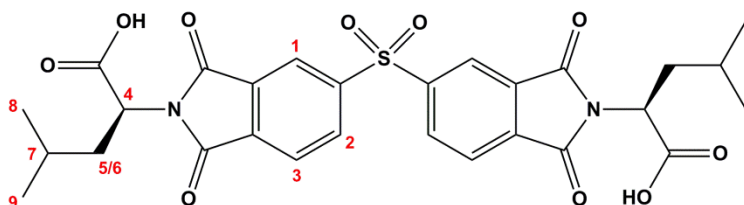
Powder X-ray diffraction (PXRD) data were collected at room temperature using a Bruker D8 Focus diffractometer equipped with Cu–K α ($\lambda = 1.5418 \text{ \AA}$) radiation. The sample was mounted on a zero background silicon single crystal stage. Data was collected in the angle interval $2\theta =$

5–55° with a step size of 0.02°. The collected data were compared to predicted patterns based on the single crystal data (collected at 100 K).

2. Synthesis

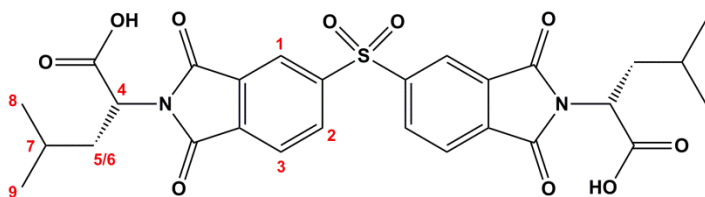
Synthesis of L-H₂LeuBPSD

A suspension of 3,3',4,4'-biphenylsulfone tetracarboxylic dianhydride (1.00 mmol, 357 mg) and L-leucine (2.10 mmol, 275 mg) in glacial acetic acid (5 mL) was heated by microwave radiation at 120 °C for 10 minutes (power input 300 W). The solution was poured over approximately 100 mL of crushed ice and allowed to stand until the ice had melted. L-H₂LeuBPSD was isolated as a white powder which was recovered by vacuum filtration, washed with water until all acid was removed and dried *in vacuo*. Yield 418 mg (72%). M.p. 159–165 °C. Found C, 54.82; H, 5.05; N, 4.77%; C₂₈H₂₈N₂O₁₀S·1.5H₂O requires C, 54.99; H, 5.11; N, 4.58%. δ_{H} (400 MHz, *d*₆-DMSO) 0.89 (d, ³*J*=7.0 Hz, 6 H, H₈,H₉), 0.91 (d, ³*J*=7.0 Hz, 6 H, H₈,H₉), 1.48 (m, 2 H, H₇), 1.89 (ddd, ²*J*=14.0 Hz, ³*J*=10.9 Hz, ³*J*=4.2 Hz, 2 H, H_{5,6}), 2.10 (ddd, ²*J*=14.0 Hz, ³*J*=10.9 Hz, ³*J*=4.2 Hz, 2 H, H_{5,6}), 4.82 (dd, ³*J*=10.9, ³*J*=4.2 Hz, 2 H, H₄), 8.16 (d, ³*J*=7.8 Hz, 2 H, H₂), 8.60 (m, 4 H, H₁, H₃). δ_{C} (100 MHz, *d*₆-DMSO) 21.3, 23.5, 24.8, 37.2, 51.0, 123.5, 125.5, 132.9, 135.2, 135.9, 145.9, 166.3, 166.5, 170.9. ν_{max} /cm⁻¹ 3993w, 3928w, 3868w, 3823w, 3747w, 3682w, 3536w, 3516w, 3486w, 3344w, 3266w, 3169w, 3052w, 2871w, 2490w, 1780w, 1719s, 1637w, 1544w, 1469w, 1383s, 1323m, 1256m, 1146m, 1104w, 1059w, 934w, 860w, 745m, 672s. *m/z* (ES⁻) 583.0 ([M-H]⁻, calculated for C₂₈H₂₇N₂O₁₀S⁻, 583.1) 100 %.



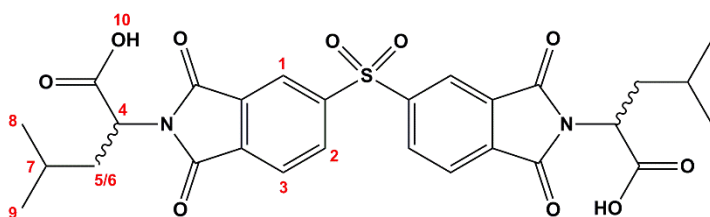
Synthesis of D-H₂LeuBPSD

A suspension of 3,3',4,4'-biphenylsulfone tetracarboxylic dianhydride (1.00 mmol, 357 mg) and D-leucine (2.10 mmol, 275 mg) in acetic acid (5 mL) was heated by microwave radiation at 120 °C for 10 minutes (power input 300 W). The solution was poured over approximately 100 mL of crushed ice and allowed to stand until the ice had melted. D-H₂LeuBPSD was isolated as a white powder which was recovered by vacuum filtration, washed with water until all acid was removed and dried *in vacuo*. Yield 461 mg (79%). M.p. 150–155 °C. Found C, 54.31; H, 4.97; N, 4.54%; C₂₈H₂₈N₂O₁₀S·2H₂O requires C, 54.19; H, 5.20; N, 4.51%. δ_{H} (400 MHz, *d*₆-DMSO) 0.84 (d, ³*J*=7.1 Hz, 6 H, H₈,H₉), 0.86 (d, ³*J*=7.1 Hz, 6 H, H₈,H₉), 1.48 (m, 2 H, H₇), 1.84 (ddd, ²*J*=14.1, ³*J*=10.8, ³*J*=4.1, 2 H, H₅,H₆), 2.14 (ddd, ²*J*=14.1, ³*J*=10.8, ³*J*=4.1, 2 H, H₅,H₆), 4.81 (dd, ³*J*=11.2, ⁴*J*=4.2, 2 H, H₄), 8.15 (dd, ³*J*=7.8, ⁴*J*=1.0, 2 H, H₂), 8.59 (m, 4 H, H₁,H₃). δ_{C} (100 MHz, *d*₆-DMSO), 21.3, 23.5, 24.8, 37.1, 51.0, 123.5, 125.5, 132.9, 135.2, 135.9, 145.9, 166.3, 166.5, 170.9. ν_{max} /cm⁻¹ 2961w, 2875w, 2629w, 2506w, 1715s, 1618w, 1469w, 1383s, 1324m, 1256m, 1145m, 1059m, 932m, 861w, 746m, 671s. *m/z* (ES⁻) 583.2 ([M-H]⁻, calculated for C₂₈H₂₇N₂O₁₀S⁻, 583.1) 100 %.



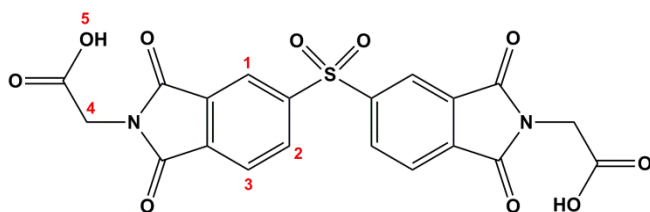
Synthesis of DL-H₂LeuBPSD

A suspension of 3,3',4,4'-biphenylsulfone tetracarboxylic dianhydride (1.00 mmol, 357 mg), D-leucine (1.05 mmol, 138 mg) and L-leucine (1.05 mmol, 138 mg) in acetic acid (5 mL) was heated at 120 °C with stirring overnight. The solution was poured over approximately 100 mL of ice and allowed to stand until the ice had melted, which caused the product to precipitate as a white powder. The product was recovered by vacuum filtration, washed with water until all acid was removed and dried *in vacuo*. Yield 526 mg (90%). M.p. 153–157 °C. Found C, 57.39; H, 4.76; N, 4.74%; C₂₈H₂₈N₂O₁₀S requires C, 57.52; H, 4.83; N, 4.79%. δ_{H} (400 MHz, *d*₆-DMSO) 0.85 (m, 12 H, H₈,H₉), 1.48 (m, 2 H, H₇), 1.85 (ddd, ²*J*=14.2, ³*J*=10.7, ³*J*=4.0 Hz, 2 H, H₅, H₆), 2.15 (ddd, ²*J*=14.2, ³*J*=10.7, ³*J*=4.0 Hz, 2 H, H₅, H₆), 4.81 (dd, ³*J*=10.7, ³*J*=4.0 Hz, 2 H, H₄), 8.15 (dd, ³*J*=7.8, ⁴*J*=1.0, 2 H, H₂), 8.59 (m, 4 H, H₁,H₃), 13.26 (br. s, 2 H, H₁₀). δ_{C} (100 MHz, *d*₆-DMSO), 21.3, 23.5, 24.8, 37.2, 51.0, 123.5, 125.5, 132.9, 135.2, 135.9, 145.9, 166.3, 166.5, 170.9. $\nu_{\text{max}}/\text{cm}^{-1}$ 2760w, 1780w, 1717s, 1616w, 1469w, 1422w, 1383s, 1323m, 1264w, 1146 μ , 1103 μ , 1059 μ , 932w, 859w, 800w, 744m, 673s. *m/z* (ES⁻) 583.1 ([M-H]⁻, calculated for C₂₈H₂₇N₂O₁₀S⁻, 583.1) 100 %.



Synthesis of H₂GlyBPSD

A suspension of 3,3',4,4'-biphenylsulfone tetracarboxylic dianhydride (1.00 mmol, 357 mg) and glycine (2.10 mmol, 158 mg) in DMF (10 mL) was heated at 100 °C with stirring overnight. The reaction was quenched by pouring onto approximately 100 mL of crushed ice and allowed to stand until all the ice had melted. H₂GlyBPSD was isolated as a white powder by vacuum filtration, washed with water (200 mL) and dried *in vacuo*. Yield 247 mg (52%). M.p. 332–336 °C. Found C, 50.78; H, 2.65; N, 5.75%; C₂₀H₁₂N₂O₁₀S requires C, 50.85; H, 2.56; N, 5.93%. δ_{H} (400 MHz, *d*₆-DMSO) 4.36 (s, 4 H, H₄), 8.18 (d, ³*J*=7.8 Hz, 2 H, H₂), 8.62 (m, 4 H, H₁,H₃), 12.7 (br, 2 H, H₅). δ_{C} (100 MHz, *d*₆-DMSO) 40.5, 123.4, 125.5, 133.2, 135.1, 136.3, 145.3, 166.0, 166.2, 169.0. ν_{max} /cm⁻¹ 3998w, 3950w, 3855w, 3713w, 3635w, 3493w, 2967w, 2900w, 2799w, 2725w, 2648w, 2546.4w, 2460 w, 2371w, 1782m, 1711s, 1528w, 1405s, 1314m, 1226m, 1146s, 1060m, 1008m, 963s, 926m, 883m, 852m, 755s, 671s. *m/z* (ES⁻) 470.9 ([M-H]⁻, calculated for C₂₀H₁₁N₂O₁₀S⁻, 471.0) 100 %.



Synthesis of Λ -[Cu₄(L-LeuBPSD)₄(OH₂)₄] \cdot 2DMA (Λ -[1(OH₂)₄] \cdot 2DMA)

Single crystals:

L-H₂LeuBPSD (10 mg, 17.1 μ mol) and Cu(NO₃)₂ \cdot 3H₂O (22 mg, 91.1 μ mol) were added to DMA (3 mL) and sonicated to dissolve. The solution was heated at 100 °C for one week in a sealed vial. The solution was then left to sit at room temperature for two months, after which time a few blue crystals formed. The X-ray data was best modelled as Λ -[Cu₄(L-LeuBPSD)₄(OH₂)₄] \cdot 2DMA. A different method was employed (see below) to synthesise a bulk sample in a reasonable timeframe for which the PXRD matched that predicted for this crystalline sample (Figure S7).

Bulk powder sample:

L-H₂LeuBPSD (100 mg, 171 μ mol) and Cu(NO₃)₂ \cdot 3H₂O (220 mg, 911 μ mol) were added to DMA (2.5 mL) and sonicated to dissolve. Methanol (4 mL) was added to the solution with stirring. A mixed solution of methanol (1 mL) and triethylamine (1 mL) was added dropwise to the metal/ligand solution with stirring until slight clouding remained (approx. 4 drops). The reaction solution was left in a capped vial overnight during which time the product formed as a blue powder which was recovered by filtration and dried in air. PXRD confirmed this material to be the same crystalline phase as that isolated as single crystals (see above and Figure S7). Yield 64 mg (56%). M.p. 282–284 °C. Found C, 51.45; H, 4.72; N, 5.22%; C₁₁₂H₁₁₂N₈O₄₄S₄Cu₄ \cdot 3.5DMA ([Cu₄(L-LeuBPSD)₄(OH₂)₄] \cdot 3.5DMA) requires C, 51.10; H, 4.89; N, 5.44%. ν_{\max} /cm⁻¹ 2954w, 1774w, 1711s, 1655m, 1610s, 1508m, 1467w, 1413m, 1377s, 1262w, 1178w, 1146m, 1102m, 1051m, 1020s, 947w, 895w, 861w, 784w, 732m, 671s. m/z (ES⁺) 2586.25 (Λ -[1+H]⁺, calculated for C₁₁₂H₁₀₅Cu₄N₈O₄₀S₄⁺, 2585.25), Figure S1. TGA: On-set, 50 °C, mass loss = 12.7 % (calculated 12.7 % for loss of 4 coordinated H₂O molecules and 3.5 non-coordinated DMA molecules), Figure S12. The best structural model that could be

fitted to the single crystal X-ray diffraction data was Λ -[Cu₄(L-LeuBPSD)₄(OH₂)₄] \cdot 2DMA with significant void space in which no solvent could be modelled. The data was processed using the SQUEEZE routine of PLATON, which showed a total void space of 1039 Å³ per unit cell (*i.e.* per cage), containing 339e⁻. This is split between a void 748 Å³ containing 318 e⁻ between the cages and a second void of 291 Å³ containing 21 e⁻ within the cage. The best fit for the TGA and microanalysis suggests the presence of four coordinated water molecules and 3.5 non-coordinated DMA molecules. The additional 1.5 DMA molecules which could not be modelled in the structure would lead to an expected 72 e⁻ per cage. The total content suggested by squeeze is 7 DMA molecules. The greater electron count suggested by SQUEEZE compared to that expected based on the TGA and microanalysis results is likely due to solvent loss upon isolation prior to TGA or microanalysis being conducted or due to some disorder that could not be modelled properly.

Synthesis of Δ -[Cu₄(D-LeuBPSD)₄(OH₂)(MeOH)_{2.5}(HNMe₂)_{0.5}] \cdot 4DMA (Δ -[1 \cdot (OH₂)(MeOH)_{2.5}(HNMe₂)_{0.5}] \cdot 4DMA)

D-H₂LeuBPSD (100 mg, 171 μ mol) and Cu(NO₃)₂ \cdot 3H₂O (220 mg, 911 μ mol) were added to DMA (2.5 mL) and sonicated to dissolve. Methanol (4 mL) was added to the solution with stirring. A mixed solution of methanol (1 mL) and triethylamine (1 mL) was added dropwise to the metal/ligand solution with stirring until slight clouding remained (approx. 3 drops). The vial was capped and left to sit for one week, after which time the product formed as blue crystals which were recovered by filtration and dried in air. Yield 62 mg (54%). M.p. 287–290 °C. Found C, 51.79; H, 5.05; N, 6.14%; C_{115.5}H_{119.5}N_{8.5}O_{43.5}S₄Cu₄ \cdot 5DMA ([Cu₄(D-LeuBPSD)₄(OH₂)(MeOH)_{2.5}(HNMe₂)_{0.5}] \cdot 5DMA) requires C, 51.8; H, 5.05; N, 6.14%. ν_{\max} /cm⁻¹ 2957w, 2871w, 1778w, 1711s, 1614s, 1469w, 1379s, 1264w, 1145s, 1103m, 1051m, 951w, 861m, 786m, 734m, 671s. Phase purity confirmed by PXRD, Fig S8. m/z (ES⁺) 2646.28 (Δ -[1(NHMe₂)(OH₂)+H]⁺, calculated for C₁₁₄H₁₁₄Cu₄N₉O₄₁S₄⁺, 2646.30), Figure S2. TGA: On-set, 25 °C, mass loss = 5.1 % (calculated 4.5 % for loss of one coordinated H₂O and 2.5 coordinated MeOH, and 0.5 coordinated HNMe₂), Figure S13. The best structural model that could be fitted to the single crystal X-ray diffraction data was Δ -[Cu₄(D-LeuBPSD)₄(OH₂)(MeOH)_{2.5}(HNMe₂)_{0.5}] \cdot 4DMA (although it is likely that the composition of the coordinated solvent is more complicated) with significant void space in which no solvent could be modelled. The diffraction data was processed using the SQUEEZE routine of PLATON which showed a voids totalling 144 Å³ and 31 e⁻ outside of the cage and voids totalling 175 Å³ and 16 e⁻ within the cage (values per cell/cage). The best fit for the microanalysis suggests the presence of one DMA molecule more than the model generated from X-ray data, which would lead to an expected 48e⁻ per cage, in line with the overall SQUEEZE results. The best fit for the TGA suggested mass loss for the coordinated solvent only. The TGA shows less mass loss than would be expected based on the single crystal

structure, SQUEEZE results and microanalysis, possibly due to solvent loss before the TGA was conducted.

Synthesis of Λ -[Cu₄(L-LeuBPSD)₄(OH₂)₂(DMSO)₂] \cdot 2DMSO (Λ -[1(DMSO)₂(OH₂)₂] \cdot 2DMSO)

An NMR sample of Λ -[Cu₄(L-LeuBPSD)₄(OH₂)₄] (5 mg) in *d*₆-DMSO (0.5 mL) was left to sit at room temperature. After one month blue crystals formed in the solution, on which X-ray diffraction data was collected. To replicate this synthesis, 83 mg of Λ 1 was dissolved in non-deuterated DMSO (1 mL) and left to sit at room temperature. After one month a microcrystalline product formed which was recovered by filtration. Found C, 45.74; H, 4.25; N, 3.69%; C₁₁₆H₁₂₀N₈O₄₄Cu₄S₆ \cdot 15H₂O ([Cu₄(L-LeuBPSD)₄(OH₂)₂(DMSO)₂] \cdot 15H₂O requires C, 45.72; H, 4.97; N, 3.68%. *m/z* (ES⁺) 2685.26, (Λ -[1(DMSO)+Na]⁺, calculated for C₁₁₄H₁₁₀Cu₄N₈O₄₁S₅Na⁺, 2685.25), Figure S3. ν_{\max} /cm⁻¹ 2733w, 1776w, 1713s, 1653m, 1616m, 1508w, 1465w, 1413m, 1379s, 1327m, 1260w, 1146m, 1101m, 1051s, 1019s, 948m, 894w, 863m, 786m, 734m, 671s. TGA: On-set, 25 °C, mass loss = 23.5 % (calculated 23.3 % for loss of 2 coordinated H₂O and 2 coordinated DMSO, and 7 DMSO and 15 H₂O), Figure S14. The best structural model that could be fitted to the single crystal X-ray diffraction data was Λ -[Cu₄(L-LeuBPSD)₄(OH₂)₂(DMSO)₂] \cdot 2DMSO with significant void space in which no solvent could be modelled. The data was processed using the SQUEEZE routine of PLATON, which showed a void space of 476 Å³ containing 148 e⁻ per cell/cage between the cages and small residual spaces within the cage (see X-ray section). TGA and microanalysis do not provide an ideal match. The best fit for the TGA data suggests the presence of two coordinated DMSO, two coordinated water molecules, 12 non-coordinated water molecules and eight non-coordinated DMSO molecules (giving an expected electron count of 328e⁻) although this is likely due to residual surface solvent on the sample and/or deliquescence. The best fit for the microanalysis suggests the presence of the two coordinated DMSO, two coordinated water molecules and 15 non-coordinated water molecules, supporting the possibility of solvent exchange and deliquescence during transport (surface water would be lost in transit).

Synthesis of Λ -[Cu₄(L-LeuBPSD)₄(MeOH)₂(OH₂)₂]/ Δ -[Cu₄(D-LeuBPSD)₄(MeOH)₂(OH₂)₂] \cdot DMA (Λ/Δ -[1(MeOH)₂(OH₂)] \cdot DMA)

L-H₂LeuBPSD (50 mg, 171 μ mol), D-H₂LeuBPSD (50 mg, 85.5 μ mol) and Cu(NO₃)₂ \cdot 3H₂O (220 mg, 911 μ mol) were added to DMA (2.5 mL) and sonicated to dissolve. Methanol (4 mL) was added to the solution with stirring. A solution of methanol (1 mL) and triethylamine (1 mL) was added dropwise to the metal/ligand solution with stirring until slight clouding remained (approx. 3 drops). The vial was capped and left to sit for one week, after which time the product formed as blue crystals which were recovered by filtration. Yield 36.1 mg (31%). M.p. 285–288 °C. Found C, 51.79; H, 5.52; N, 6.84%; C₁₁₄H₁₁₆N₈O₄₄S₄Cu₄ \cdot 8DMA, ([Cu₄(LeuBPSD)₄(MeOH)₂(OH₂)₂] \cdot 8DMA) requires C, 51.85; H, 5.61; N, 6.63%. ν_{\max} /cm⁻¹ 2957w, 2871w, 1778w, 1711s, 1611m, 1469w, 1379s, 1148m, 1103m, 1051m, 947m, 861w, 786w, 734s, 671s. Phase purity confirmed by PXRD, Fig S9. m/z (ES⁻) 2619.22 (Λ/Δ -[1+Cl]⁻, calculated for C₁₁₂H₁₀₄Cu₄N₈O₄₀S₄Cl⁻, 2619.21), 2629.29 (Λ/Δ -[1(NHMe₂)+H]⁺, calculated for C₁₁₄H₁₁₂Cu₄N₉O₄₀S₄⁻, 2628.29), 2646.28 (Λ/Δ -[1(NHMe₂)(OH₂)+H]⁺, calculated for C₁₁₄H₁₁₃Cu₄N₉O₄₁S₄⁻, 2646.30), Figure S4. TGA: On-set, 25 °C, mass loss = 18.0 % (calculated 18.4 % for loss of 2 coordinated MeOH and 2 coordinated H₂O, and 5 non-coordinated DMA and 1 non-coordinated MeOH), Figure S15. The best structural model that could be fitted to the single crystal X-ray diffraction data was Λ -[Cu₄(L-LeuBPSD)₄(MeOH)₂(OH₂)₂]/ Δ -[Cu₄(D-LeuBPSD)₄(MeOH)₂(OH₂)₂] \cdot DMA (although it is likely that the composition of the coordinated solvent is more complicated with some HNMe₂ present at low occupancy that could not be refined) with significant void space in which no solvent could be modelled. The data was processed using the SQUEEZE routine of PLATON which showed voids between the cages (896 Å³ and 235 e⁻ per cage) and a void of 293 Å³ containing 65 e⁻ inside each cage. The mass spectrum shows two peaks corresponding to the cage containing one coordinated water molecule and one dimethylamine, and one dimethylamine. Although NHMe₂ could not be

modelled in the single crystal X-ray structure, dimethylamine was present from hydrolysis of DMA used in the reaction and is likely present in the crystalline sample with the cages containing various compositions of solvent and the average electron density not being sufficient to resolve this mixture, although Λ/Δ -[**1**(NHMe₂)+H]⁺ and Λ/Δ -[**1**(NHMe₂)(OH₂)+H]⁺ may represent two of the most stable ions which could be observed in the mass spectra. The best fit for the TGA analysis suggests the presence of two coordinated MeOH, two coordinated H₂O and five noncoordinated DMA and one noncoordinated MeOH. The best fit for the microanalysis is in close agreement and suggests the presence of two coordinated MeOH, two coordinated H₂O and five noncoordinated DMA molecules. The solvent not modelled in the crystal structure which is observed in the TGA and the microanalysis corresponds to an electron count of 322e⁻ and 336e⁻, respectively, which is in rough agreement with the SQUEEZE results given the complicated mixture of potential solvents in the material.

Synthesis of $[\text{Cu}_4(\text{DL-H}_2\text{LeuBPSD})_4(\text{OH}_2)_2(\text{MeOH})_2]\cdot 2\text{DMA}$, $([\text{2}(\text{OH}_2)_2(\text{MeOH})_2]\cdot 2\text{DMA})$

rac-H₂LeuBPSD (100 mg, 85.5 μmol) and Cu(NO₃)₂·3H₂O (220 mg, 911 μmol) were added to DMA (2.5 mL) and stirred to dissolve. Methanol (4 mL) was added to the solution with stirring. A solution of methanol (1 mL) and triethylamine (1 mL) was added dropwise to the metal/ligand solution with stirring until slight clouding remained (approx. 3 drops). The vial was capped and left to sit for four nights, after which time the product formed as blue crystals which were recovered by filtration. Yield 27.4 mg (22%). M.p. 271–273 °C. Found C, 51.12; H, 4.70; N, 5.04%; C₁₁₄H₁₁₆N₈O₄₄S₄Cu₄·2.5DMA, ([Cu₄(DL-H₂LeuBPSD)₄(OH₂)₂(MeOH)₂]₂·2.5DMA requires C, 51.13; H, 4.81; N, 5.07%. ν_{max}/cm⁻¹ 2200w, 1776w, 1717s, 1646m, 1608m, 1506w, 1467w, 1413m, 1381s, 1351m, 1323s, 1264w, 1142m, 1105m, 1057m, 1014w, 939w, 909w, 863w, 784m 745m, 671s. Phase purity confirmed by PXRD, Fig S10. *m/z* (ES⁺) 2607.19 ([2+Na]⁺, calculated for C₁₁₂H₁₀₄Cu₄N₈O₄₀S₄Na⁺, 2607.23), 2685.40 ([2(MeOH)₂(OH₂)₂+H]⁺, calculated for C₁₁₄H₁₁₇Cu₄N₈O₄₄S₄⁺, 2685.32), Figure S5. TGA: On-set, 25 °C, mass loss = 23.3 % (calculated 23.6 % for loss of 2 coordinated H₂O and 2 coordinated MeOH, and 8 DMA), Figure S16. The best structural model that could be fitted to the single crystal X-ray diffraction data was [Cu₄(DL-H₂LeuBPSD)₄(OH₂)₂(MeOH)₂]₂·2DMA with significant void space in which no solvent could be modelled. The data was processed using the SQUEEZE routine of PLATON, which showed a void space of 1183 Å³ per unit cell (*i.e.* per cage), containing 280e⁻ per cage. The best fit for the TGA data suggests the presence of the two coordinated methanol, two coordinated water molecules and eight DMA molecules. The six additional non-coordinated DMA molecules suggested by the TGA would correspond to 264e⁻ which is in reasonable agreement with SQUEEZE. The best fit for the microanalysis suggests the presence of the two coordinated methanol, two coordinated water molecules and two non-coordinated DMA molecules. The

lower solvent content suggested by the microanalysis results is likely due to solvent loss upon isolation and transport prior to the microanalysis being conducted.

Synthesis of $[\text{Cu}_4(\text{GlyBPSD})_4(\text{MeOH})_3(\text{OH}_2)] \cdot 3.5\text{DMA} \cdot 1.5\text{MeOH}$

$([\mathbf{3}(\text{MeOH})_3(\text{OH}_2)] \cdot 3.5\text{DMA} \cdot 1.5\text{MeOH})$

Single crystals:

$\text{H}_2\text{GlyBPSD}$ (10 mg, 21.2 μmol) was dissolved in DMA (0.5 mL). $\text{Cu}(\text{NO}_3)_2 \cdot 3\text{H}_2\text{O}$ (15.4 mg, 63.6 μmol) was also dissolved in DMA (0.5 mL) and combined with the ligand solution. Methanol (1 mL) was added to the combined metal/ligand solution with stirring. A solution of triethylamine (3 drops) in methanol (5 mL) was added dropwise to the metal/ligand solution with stirring, until the solution became cloudy (~0.5 mL). When the solution became cloudy the vial was capped and left to sit for one month, after which time a few blue crystals, suitable for X-ray diffraction formed. The X-ray data was best modelled as $[\text{Cu}_4(\text{GlyBPSD})_4(\text{MeOH})_3(\text{OH}_2)] \cdot 3.5\text{DMA} \cdot 1.5\text{MeOH}$. A different method was employed (see below) to synthesise a bulk sample in reasonable timeframe for which the PXRD matched that predicted for this crystalline sample (Figure S11).

Bulk powder sample:

$\text{H}_2\text{GlyBPSD}$ (30 mg, 63.6 μmol) and $\text{Cu}(\text{NO}_3)_2 \cdot 3\text{H}_2\text{O}$ (46.2 mg, 190.7 μmol) were dissolved in a mixture of DMA (3 mL) and methanol (3 mL). A solution of triethylamine (3 drops) in methanol (5 mL) was added dropwise with stirring until the blue solution became slightly cloudy (approx. 2 mL). A blue powder was isolated by filtration after three nights, with PXRD confirming it to be the same crystalline phase as that isolated as single crystals (see above and Figure S11). Yield 25.0 mg (69%). M.p. >350 °. Found C, 41.00; H, 2.87; N, 4.89%; $\text{C}_{83}\text{H}_{54}\text{N}_8\text{O}_{44}\text{S}_4\text{Cu}_4 \cdot 4\text{H}_2\text{O} \cdot 6\text{MeOH}$ ($[\text{Cu}_4(\text{GlyBPSD})_4(\text{MeOH})_3(\text{OH}_2)] \cdot 4\text{H}_2\text{O} \cdot 6\text{MeOH}$) requires C, 41.02; H, 3.07; N, 4.61%. $\nu_{\text{max}} / \text{cm}^{-1}$ 1775s, 1707s, 1593s, 1411s, 1372s, 1318s, 1198s, 1146s, 1061m, 1003m, 969s, 930m, 887w, 802w, 749s, 712s, 675s. m/z (ES^+) 2136.74 ($[\mathbf{3}+\text{H}]^+$, calculated for $\text{C}_{80}\text{H}_{41}\text{Cu}_4\text{N}_8\text{O}_{40}\text{S}_4^+$, 2136.75), 2168.77 ($[\mathbf{3}+\text{MeOH}+\text{H}]^+$, calculated for

$C_{81}H_{45}Cu_4N_8O_{41}S_4^+$, 2168.77), Figure S6. TGA: On-set, 25 °C mass loss = 18.6% (calculated 18.6 % for loss of 3 coordinated MeOH and 1 H₂O, and 4 non-coordinated H₂O, 7 MeOH and 2 DMA), Figure S17. The best structural model that could be fitted to the single crystal X-ray diffraction data was $[Cu_4(GlyBPSD)_4(MeOH)_3(OH_2)] \cdot 3.5DMA \cdot 1.5MeOH$. There is some variation in the degree and composition of solvation in the single crystal structure and that suggested by TGA and microanalysis. This is likely due to the slight difference in synthetic conditions, some disorder associated with solvent molecules in the crystal structure (see X-Ray crystallography details) and handling methods for the various analyses. TGA suggests the presence of more solvent than the microanalysis results, with loss of solvent likely in transit.

3. X-Ray Crystallography Details

Data for all structures was collected using the MX1 beamlines at the Australian Synchrotron (all but $\Lambda 1$) or a Bruker ApexII diffractometer ($\Lambda 1$).

Data collected using the Bruker ApexII diffractometer were collected at 123 K using graphite monochromated Mo-K α radiation ($\lambda = 0.71073 \text{ \AA}$). Data collection and processing was conducted using the SAINT software suite.¹

Data collected using the Australian Synchrotron were collected at 100 K using an energy equivalent to Mo-K α radiation (17.4 keV, $\lambda = 0.7108 \text{ \AA}$). Data collection was controlled using the BluIce software package.² Data indexing and integration were conducted using the program XDS.³

All structures were solved by direct methods using SHELXS⁴ or SHELXT⁵ and refined with SHELXL-2014⁶ using Olex2 as an interface.⁷ Non-hydrogen atoms were refined with anisotropic displacement parameters with some exceptions in instances of disorder (see details below, most structures suffer from disordered leucine side-chains and significant solvent voids between cages). Hydrogen atoms attached to carbon were placed in calculated positions and refined using a riding model with isotropic displacement parameters 1.2 or 1.5 times the isotropic equivalent of their carrier atoms. Where possible hydrogen atoms attached to oxygen or nitrogen (*i.e.* in H₂O, MeOH or HNMe₂) were located from the Fourier difference map and refined with appropriate restraints and with isotropic parameters 1.5 times the isotropic equivalent of their carrier atoms. All structures had some difficulty in the refinement due to disordered alkyl chains or solvent (most involving SQUEEZE)⁸ and specific refinement details pertinent to individual structures are given below.

Table 1: Crystallographic Information

Compound	Λ-[Cu₄(L-LeuBPSD)₄(OH₂)₄]\cdot2 DMA	Δ-[Cu₄(D-LeuBPSD)₄(OH₂)(MeOH)₂.5(HNMe₂)_{0.5}]\cdot4DMA	Λ-[Cu₄(L-LeuBPSD)₄(OH₂)₂(d₆-DMSO)₂]\cdot2d₆-DMSO	Λ/Δ-[Cu₄(D/L-LeuBPSD)₄(MeOH)₂(OH₂)₂]\cdotDMA	[Cu₄(DL-H₂LeuBPSD)₄(OH₂)₂(MeOH)₂]\cdot2DMA	[Cu₄(GlyBPSD)₄(MeOH)₃(OH₂)]\cdot3.5DMA\cdot1.5MeOH
Compound abbreviation	Λ-1	Δ-1	Λ-1(DMSO)	Λ/Δ-1	2	3
Chemical formula	C ₁₂₀ H ₁₃₀ Cu ₄ N ₁₀ O ₄₆ S ₄	C _{131.5} H ₁₅₆ Cu ₄ N _{12.5} O _{47.5} S ₄	C ₁₂₀ H ₁₀₈ D ₂₄ Cu ₄ N ₈ O ₄₆ S ₈	C ₁₁₈ H ₁₂₅ Cu ₄ N ₉ O ₄₅ S ₄	C ₁₂₂ H ₁₃₄ Cu ₄ N ₁₀ O ₄₆ S ₄	C _{98.5} H _{91.5} Cu ₄ N _{11.5} O ₄₉ S ₄
Formula Mass	2917.85	3033.03	2957.12	2771.66	2858.78	2601.72
Crystal system	triclinic	triclinic	triclinic	monoclinic	triclinic	monoclinic
Space group	<i>P</i> 1	<i>P</i> 1	<i>P</i> 1	<i>C</i> 2/ <i>c</i>	<i>P</i> -1	<i>P</i> 2 ₁ / <i>n</i>
<i>a</i> /Å	15.722(3)	15.702(3)	15.638(3)	33.892(4)	14.751(3)	16.094(3)
<i>b</i> /Å	15.738(3)	15.714(3)	15.8320(6)	15.712(3)	17.672(4)	20.448(4)
<i>c</i> /Å	18.629(4)	18.656(4)	18.4820(19)	62.235(8)	19.460(4)	20.371(4)
α /°	104.90(3)	113.620(3)	72.648(7)	90	102.82(3)	90
β /°	114.87(3)	107.650(7)	65.229(3)	104.151(5)	107.63(3)	101.20(3)
γ /°	91.30(3)	90.700(7)	89.532(12)	90	106.68(3)	90
Unit cell volume/Å ³	3996.1(17)	3971.6(9)	3929.5(17)	32135(8)	4358.1(19)	6576(2)
Temperature/K	123(2)	100(2)	100(2)	100(2)	100(2)	100(2)
Z	1	1	1	8	1	2
No. of reflections measured (<i>R</i> _{int})	86893 (0.0462)	132655 (0.0525)	101474 (0.0588)	253460 (0.0754)	144847 (0.1208)	61243 (0.0645)
No. of independent reflections	31934	36094	36907	37475	20739	15590
Final <i>R</i> ₁ values (<i>I</i> > 2σ(<i>I</i>)/all data)	0.0716/0.1296	0.0660/0.0736	0.0896/0.1031	0.1148/0.1245	0.0873/0.1069	0.0719/0.0758
Final w <i>R</i> (<i>F</i> ²) values (<i>I</i> > 2σ(<i>I</i>))	0.1882	0.1874	0.2614	0.2806	0.2474	0.2198
Final w <i>R</i> (<i>F</i> ²) values (all data)	0.2291	0.1967	0.2814	0.2863	0.2665	0.2238
Flack parameter ⁹	0.016(5)	0.029(3)	0.049(4)	-	-	-

Δ -[Cu₄(L-LeuBPSD)₄(OH₂)₄] \cdot 2DMA

Side chains of three of the leucine groups were modelled over two positions with freely refined occupancies (84:16), (39:61) and (21:79). Each of these disordered groups was refined using a combination of SHELX DELU, SIMU, RIGU, ISOR and DFIX restraints. One of these disordered chains shows further signs of disorder that could not be modelled and therefore elongated anisotropic displacement parameters have been left in this fragment (C24-C27) as the best descriptor of the disorder. One of the DMA molecules which could be located in the lattice was refined using DELU restraints. The coordinated water molecules are refined with a fixed geometry free to rotate around the O-Cu bond.

The structural data was processed with the SQUEEZE routine of PLATON. A void of 748 Å³ containing 318 e⁻ was identified between the cages. A second void of 291 Å³ containing 21 e⁻ was identified inside each cage. (Note, there is one cage per unit cell). See synthetic section for details of solvent assignment.

Δ -[Cu₄(D-LeuBPSD)₄(OH₂)(MeOH)_{2.5}(HNMe₂)_{0.5}] \cdot 4DMA

The best model for solvent coordinated to the inside of the cage was H₂O and MeOH (50:50) coordinated to Cu₃ and HNMe₂ and H₂O (50:50) coordinated to Cu₂ (dimethylamine indicated by mass spectrometry results). For Cu₃, the carbon atom of the 50% occupancy coordinated MeOH was modelled over two positions, each at 25% occupancy and the hydrogen atoms on the oxygen atom coordinated to Cu₃ could not be located (but are included in the formula unit). The partial occupancy carbon and nitrogen atoms of the coordinated MeOH and HNMe₂ within the cage were refined with ISOR restraints due to what appears to be further rotation around the Cu-O/N bond that could not be resolved. One disordered side-chain of a leucine group was modelled over two positions (57:43). Two other side-chains show signs of disorder which could not be modelled (evidenced by elongated displacement parameters) and were refined using SHELXL DELU restraints. The best model of non-coordinated solvent was of four DMA molecules, one of which is modelled as disordered over two non-overlapping positions (43:57). One of the full occupancy DMA molecules shows signs of disorder which could not be modelled therefore one of the carbon atoms (C125) was refined with a SHELX ISOR restraint.

The structural data was treated with the SQUEEZE routine of PLATON. One significant void was identified between complexes (totalling 144 Å³ and 31 e⁻ per cell/cage) in addition to two

small voids (9 and 16 Å³) with no calculated electron density. The void space inside the cage was output by SQUEEZE as several small voids around the coordinated solvent (significant voids of 70 Å³ and 8 e⁻, 44 Å³ and 4 e⁻, 40 Å³ and 3 e⁻ per cage and a total, including smaller spaces, of totalling 175 Å³ and 16 e⁻). These voids sit around the internally coordinated solvent as modelled and are highly unlikely to be discrete voids except when viewed as this stationary model. See synthetic section for details of solvent assignment.

Λ-[Cu₄(L-LeuBPSD)₄(OH₂)₂(DMSO)₂]·2DMSO****

The best model for coordinated solvent was H₂O coordinated to the external sites and DMSO coordinated to the internal sites. The two internal DMSO molecules were modelled as disordered over two positions with refined occupancies tied to each other (53:47) and some bond distance and RIGU restraints applied. Four half occupancy DMSO sites were located in the lattice and were refined anisotropically with some restraints on bond lengths and displacement parameters. The side chains of some of the leucine groups show signs of disorder (evidenced from large displacement parameters) which could not be resolved and were therefore refined with some DFIX, RIGU and ISOR restraints.

The structural data was processed with the SQUEEZE routine of PLATON. Voids totalling 476 Å³ containing 148 e⁻ per cell/cage were identified between the cages and two small voids (28 Å³ and 3 e⁻; 27 Å³ and 3 e⁻) were located within the cage (likely due to unresolvable disorder rather than other solvent molecules given low e⁻ count).

Λ/Δ-[Cu₄(D/L-LeuBPSD)₄(MeOH)₂(OH₂)₂]·DMA****

Hydrogen atoms attached to H₂O and MeOH were located from the Fourier difference map and refined with restrained OH distances. There is minor residual electron density in the interior of the cage that suggests MeOH or HNMe₂ may be coordinated but at very low occupancy and therefore this could not be modelled. Several leucine side-chains show signs of disorder that could not be modelled and were refined using SHELXL SADI and SIMU restraints with elongated displacement parameters left in the final refinement model as the best descriptor for the disorder. One of the leucine groups is modelled over two positions (occupancies refined to 47:53) with one of the positions showing signs of further disorder that could not be modelled

and therefore elongated displacement parameters for this group (C112-114, with weak ISOR restraints) have been left in the model as the best descriptor for the disorder.

The structural data was processed with the SQUEEZE routine of PLATON. Voids totalling 7166 Å³ containing 1878 e⁻ per unit cell were identified between the cages (896 Å³ and 235 e⁻ per cage) and a void of 293 Å³ containing 65 e⁻ was identified inside each cage. See synthetic section for details of solvent assignment.

[Cu₄(DL-H₂LeuBPSD₄)(OH₂)₂(MeOH)₂]·2DMA****

Whilst being of slightly low quality the data is the best that could be achieved from the samples. The lattice solvent is modelled as two partial occupancy DMA sites with occupancies refined against each other (51:49) per asymmetric unit (*i.e.* total of complete 2 DMA molecules per cage). DFIX and DELU restraints were used in the refinement of these partial occupancy solvent molecules. OH hydrogen atoms were located from the Fourier difference map and refined with a restrained OH distance.

The structural data was treated with the SQUEEZE routine of PLATON. A void of 1180 Å³ and 280 e⁻ per unit cell (*i.e.* per cage) was identified which exists between the cages. See synthetic section for details of solvent assignment.

[Cu₄(GlyBPSD)₄(MeOH)₃(OH₂)]·3.5DMA·1.5MeOH****

Coordinated solvent was best modelled as a full occupancy MeOH on Cu1 (inside the cage) and 50:50 MeOH:H₂O on the exterior sites. This exterior MeOH was modelled as disordered over two positions with H atom positions restrained by DFIX whilst the hydrogen atoms of the partial occupancy water could not be modelled (but are included in the molecular formula). Lattice solvent was best modelled as one half occupancy DMA molecules, one half occupancy MeOH and one quarter occupancy MeOH per asymmetric unit (*i.e.* per half cage). Non-coordinated solvent within the cage was best modelled as one half occupancy DMA and one three-quarter occupancy DMA that is refined over two disordered positions (fixed 25:50 occupancies). Some DFIX, DELU and ISOR restraints were applied to the partial occupancy solvent positions. There is a very small void in the structure (50 Å³) which is considered too small to be treated with SQUEEZE.

4. Mass Spectrometry

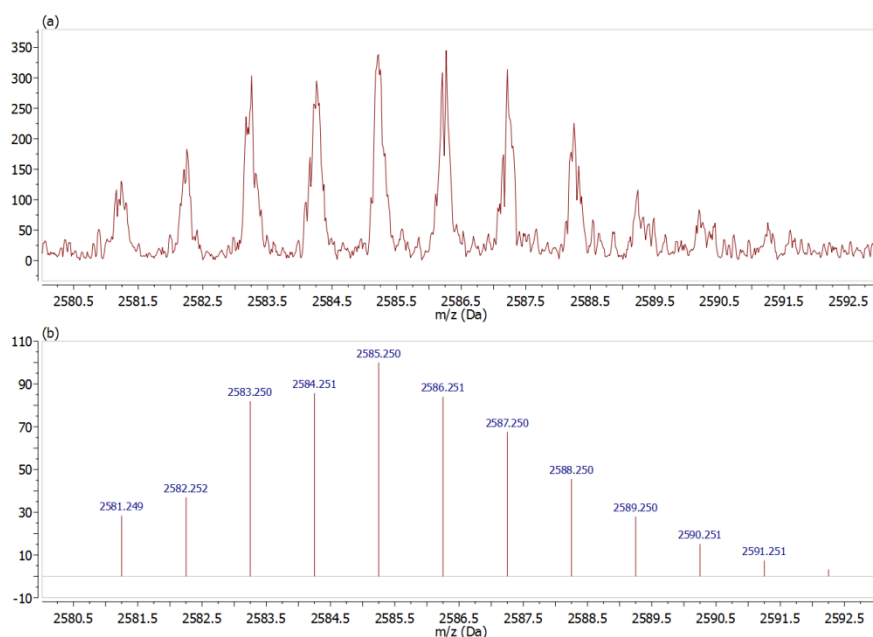


Figure S1: Magnified section of mass spectrum of $\Delta 1$. (a) Experimental $[\Delta 1+H]^+$, (b) calculated $[\Delta 1+H]^+$.

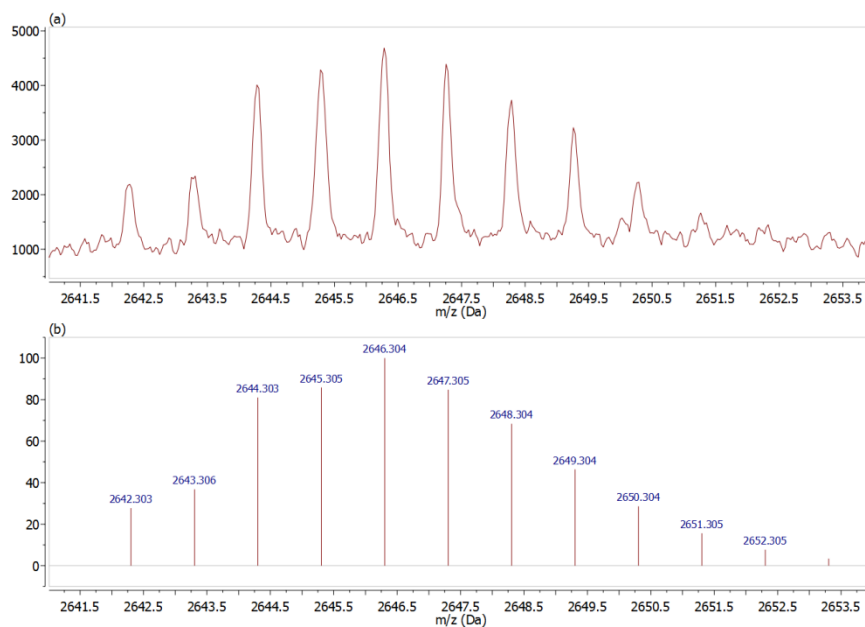


Figure S2: Magnified section of mass Spectra of $\Delta 1$. (a) Experimental $[\Delta 1+NHMe_2+H_2O-H]^-$, (b) calculated $[\Delta 1+NHMe_2+H_2O-H]^-$.

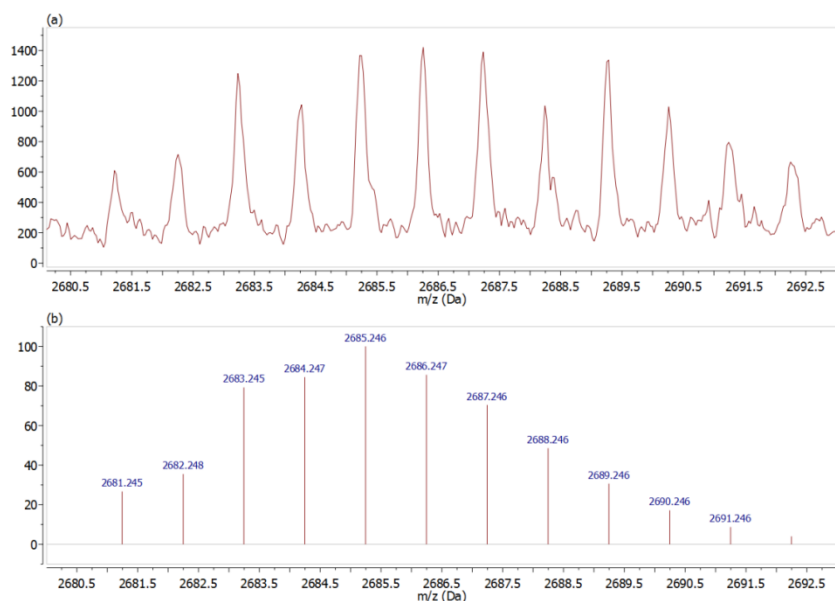


Figure S3: Magnified section of mass spectra of Λ -[Cu₄(L-LeuBPSD)₄(OH₂)₂(DMSO)₂] \cdot 2DMSO. (a) Experimental [Λ 1+DMSO+Na]⁺, (b) calculated [Λ 1+DMSO+Na]⁺.

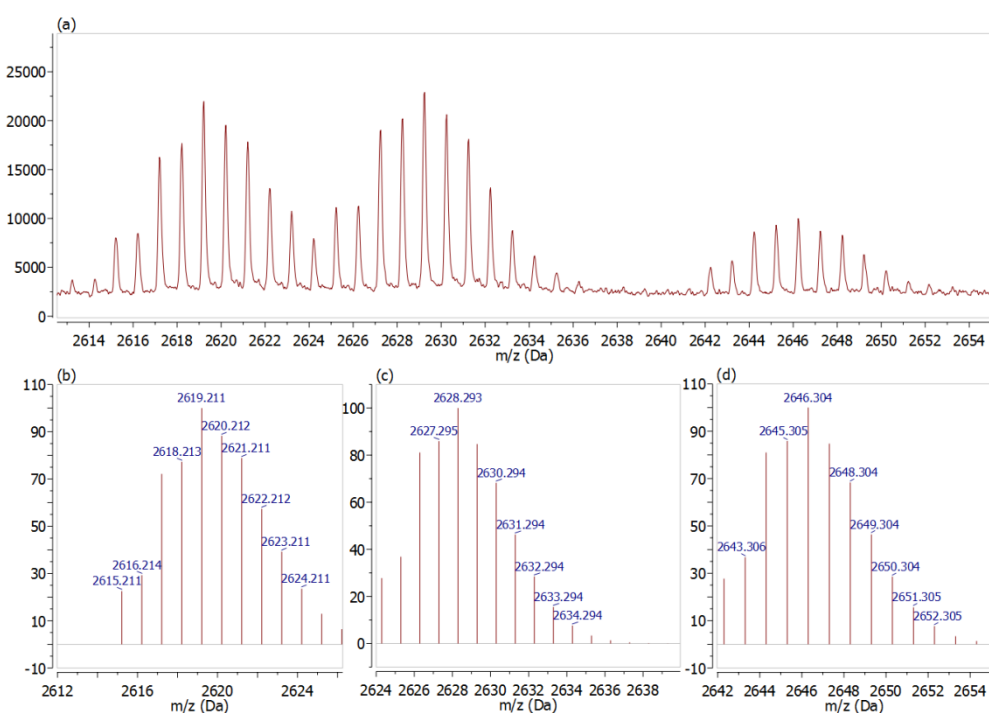


Figure S4: Magnified section of mass Spectrum of Δ/Λ -1. (a) Experimental, (b) calculated [Δ/Λ -1+Cl]⁻, (c) calculated [Δ/Λ -1+ NHMe₂-H]⁻, (d) calculated [Δ/Λ -1+ NHMe₂+H₂O-H]⁻.

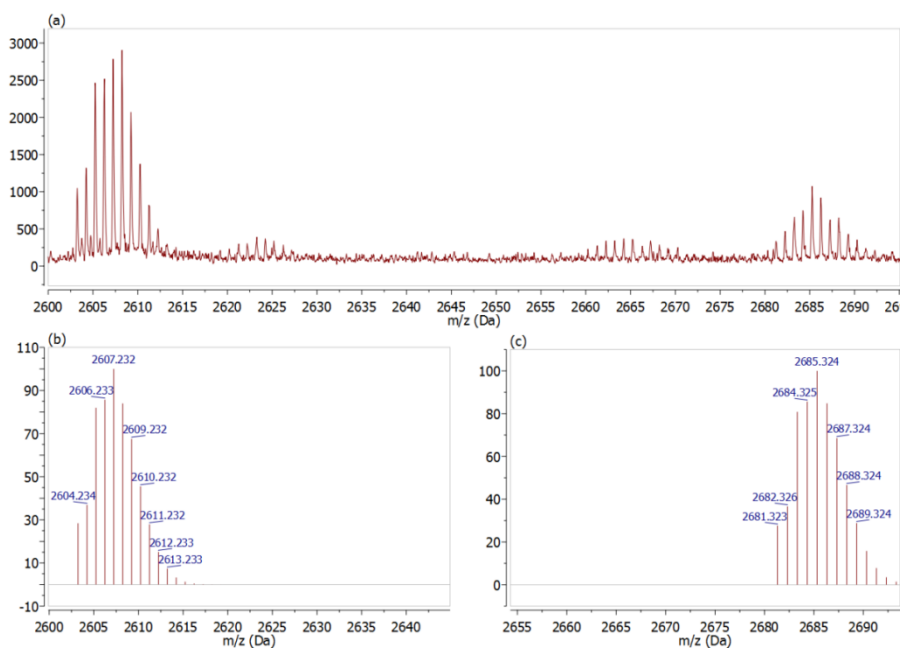


Figure S5: Magnified section of mass Spectra of **2**. (a) Experimental $[2(\text{MeOH})_2(\text{OH})_2+\text{H}]^+$ and $[2(\text{MeOH})_2(\text{OH})_2+\text{Na}]^+$, (b) calculated $[2(\text{MeOH})_2(\text{OH})_2+\text{H}]^+$, (c) experimental $[2(\text{MeOH})_2(\text{OH})_2+\text{Na}]^+$.

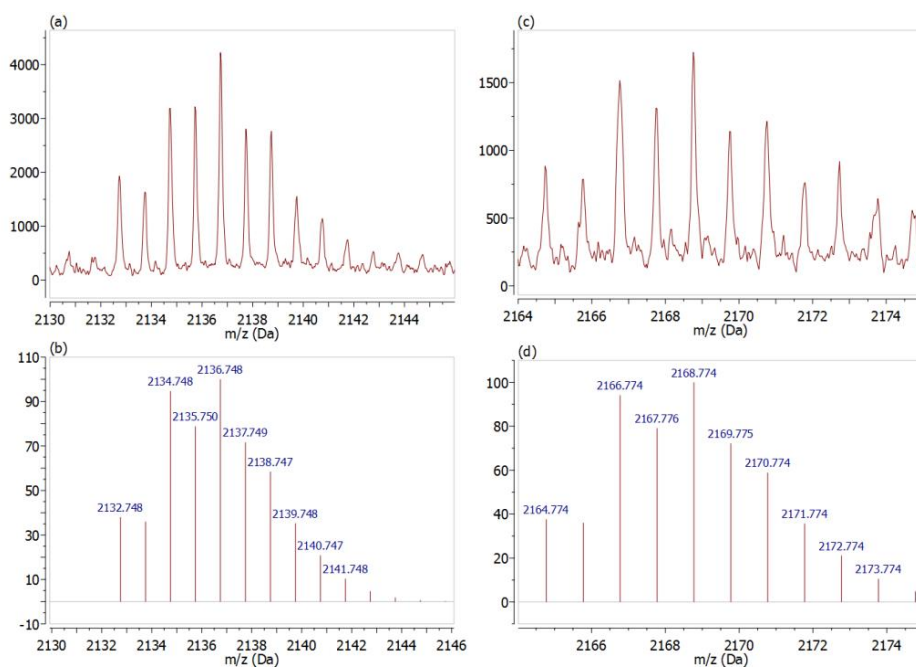


Figure S6: Magnified section of mass Spectra of **3**. (a) Experimental $[3+\text{H}]^+$, (b) calculated $[3+\text{H}]^+$, (c) experimental $[3+\text{MeOH}+\text{H}]^+$, (d) calculated $[3+\text{MeOH}+\text{H}]^+$.

5. Powder X-Ray Diffraction

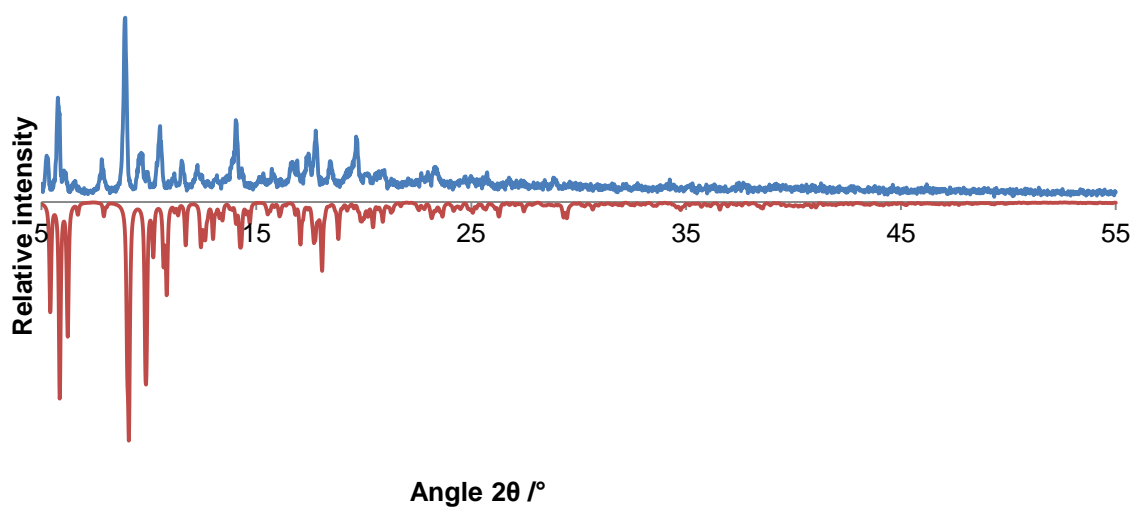


Figure S7: Comparison of experimental (298 K, blue) and calculated (100 K, red) PXRD of Λ -[Cu₄(L-LeuBPSD)₄(OH₂)₄] \cdot 2DMA.

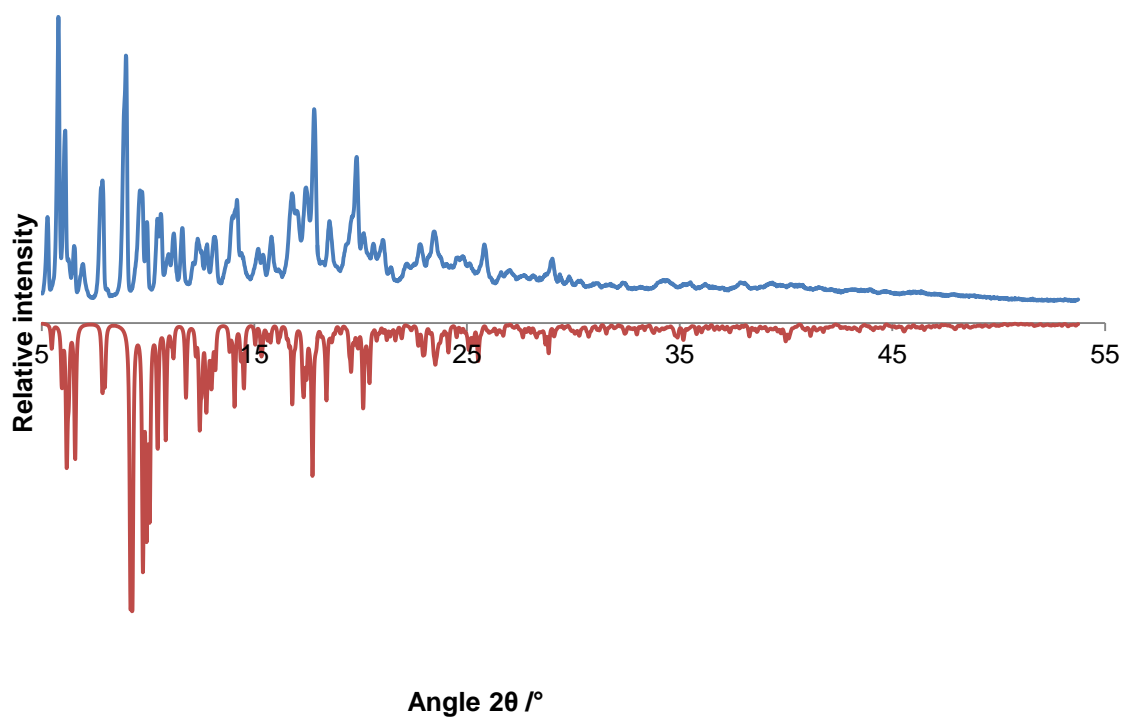


Figure S8: Comparison of experimental (298 K, blue) and calculated (100 K, red) PXRD of Λ -[Cu₄(D-LeuBPSD)₄(OH₂)(MeOH)_{2.5}(HNMe₂)_{0.5}] \cdot 3DMA.

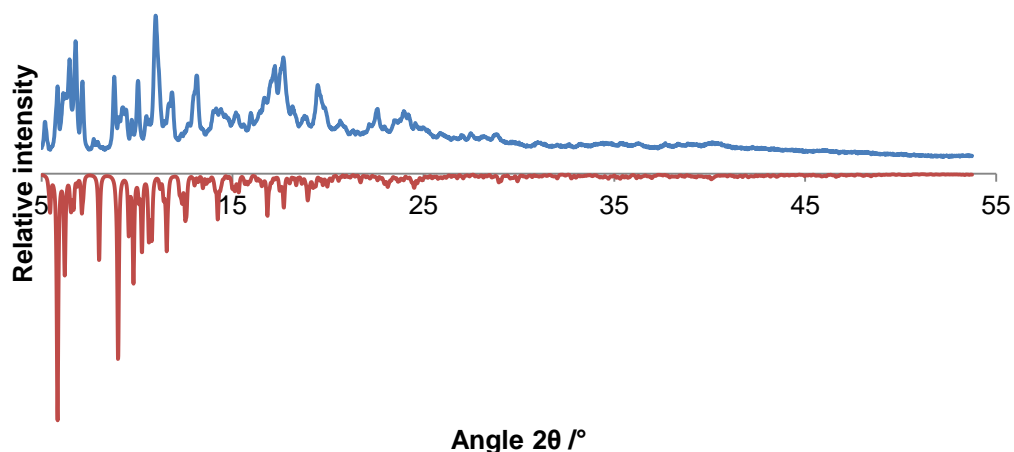


Figure S9: Comparison of experimental (298 K, blue) and calculated (100 K, red) PXRD of Λ -[Cu₄(L-LeuBPSD)₄(MeOH)₂(OH₂)₂]/ Δ -[Cu₄(D-LeuBPSD)₄(MeOH)₂(OH₂)₂] \cdot DMA.

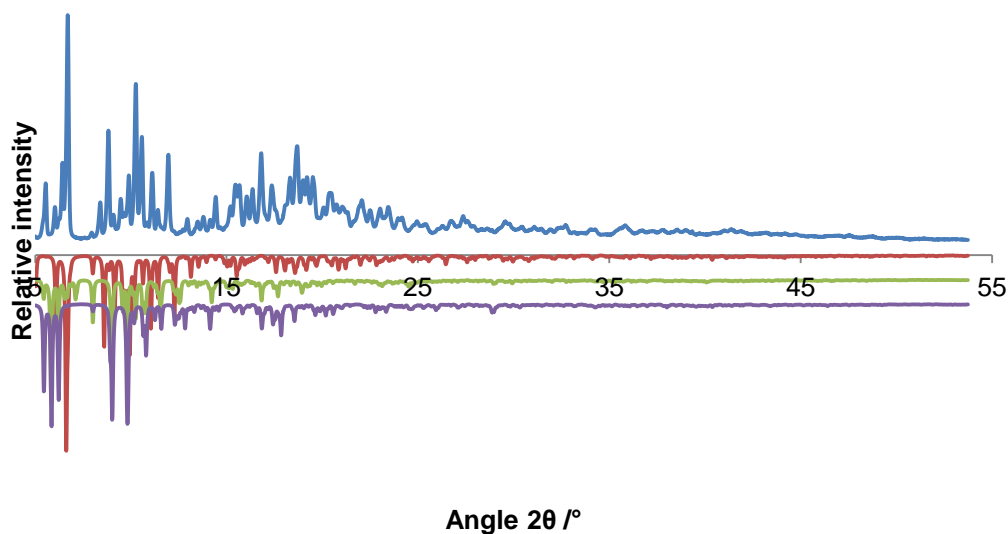


Figure S10: Comparison of experimental (298 K) PXRD pattern of [Cu₄(DL-H₂LeuBPSD)₄(OH₂)₂(MeOH)₂] \cdot 2DMA (blue) and calculated (100 K) PXRD of [Cu₄(DL-H₂LeuBPSD)₄(OH₂)₂(MeOH)₂] \cdot 2DMA (red), Λ -[Cu₄(L-LeuBPSD)₄(MeOH)₂(OH₂)₂]/ Δ -[Cu₄(D-LeuBPSD)₄(MeOH)₂(OH₂)₂] \cdot DMA (green) and Λ -[Cu₄(L-LeuBPSD)₄(OH₂)₄] \cdot 3DMA (purple).

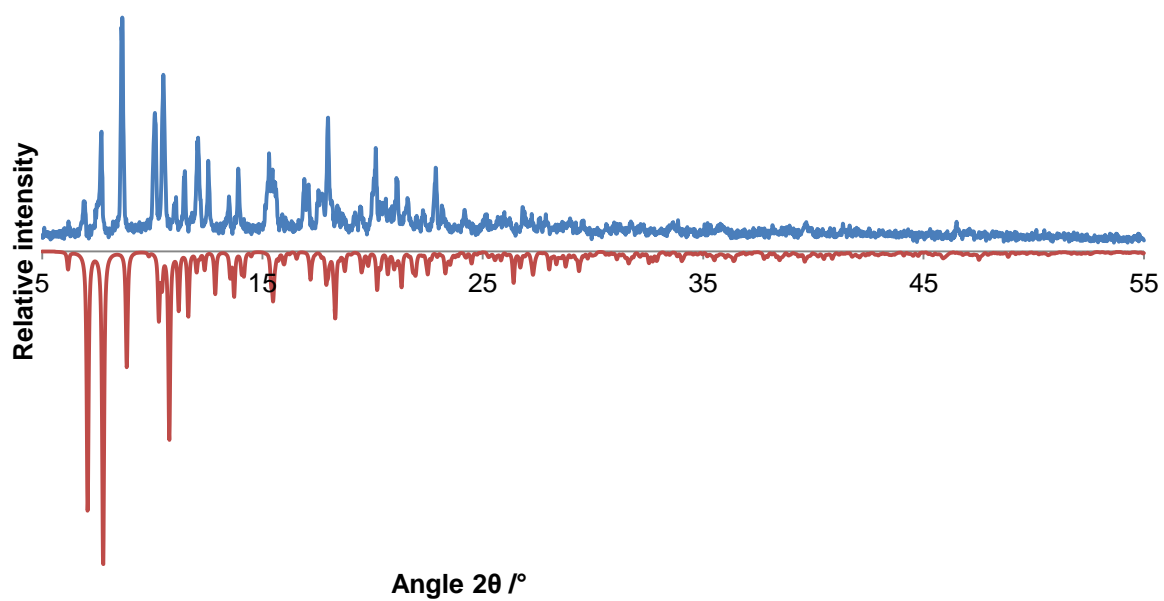


Figure S11: Comparison of experimental (298 K, blue) and calculated (100 K, red) PXRD patterns of $[\text{Cu}_4(\text{GlyBPSD})_4(\text{MeOH})_3(\text{OH}_2)] \cdot 3.5\text{DMA} \cdot 1.5\text{MeOH}$.

6. Thermogravimetric Analysis

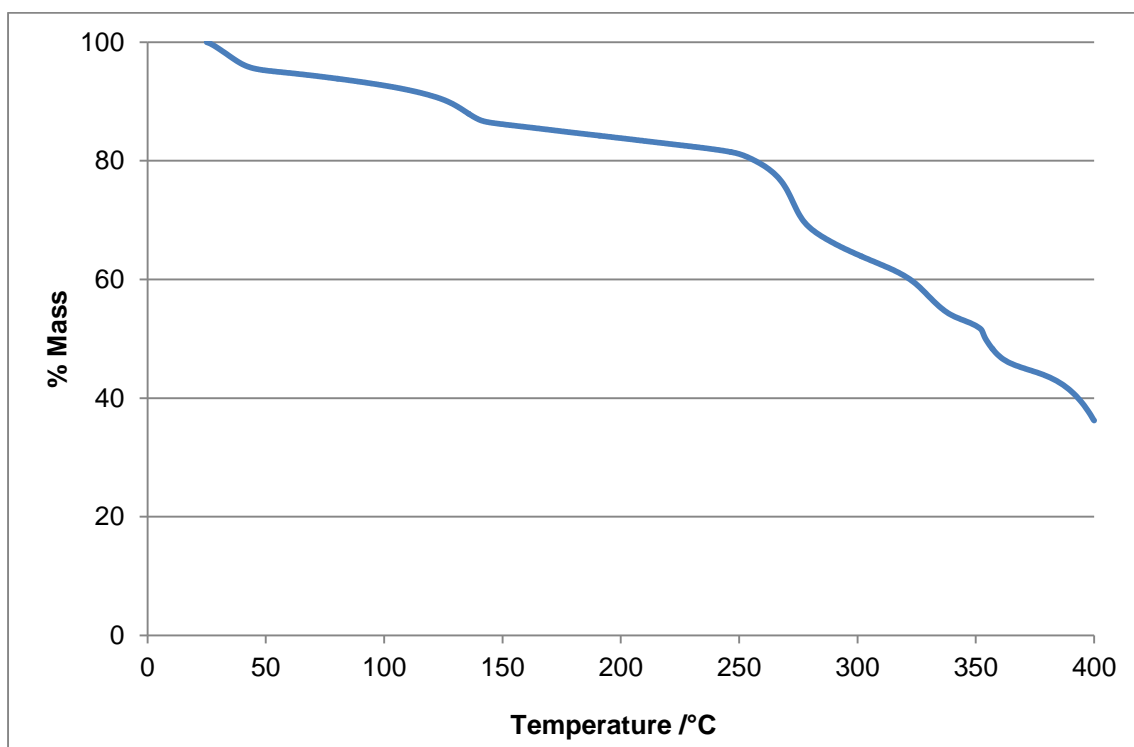


Figure S12: Thermogravimetric analysis trace for Λ -[Cu₄(L-LeuBPSD)₄(OH₂)₄]·2DMA.

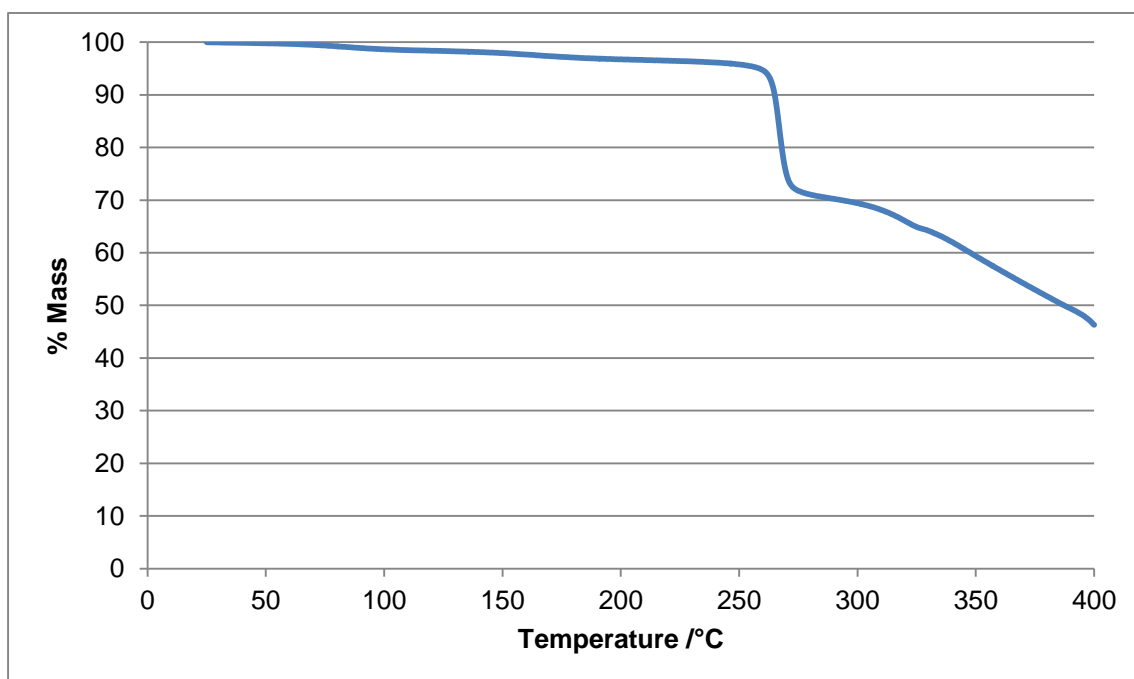


Figure S13: Thermogravimetric analysis trace for Δ -[Cu₄(D-LeuBPSD)₄(OH₂)(MeOH)_{2.5}(HNMe₂)_{0.5}]·4DMA.

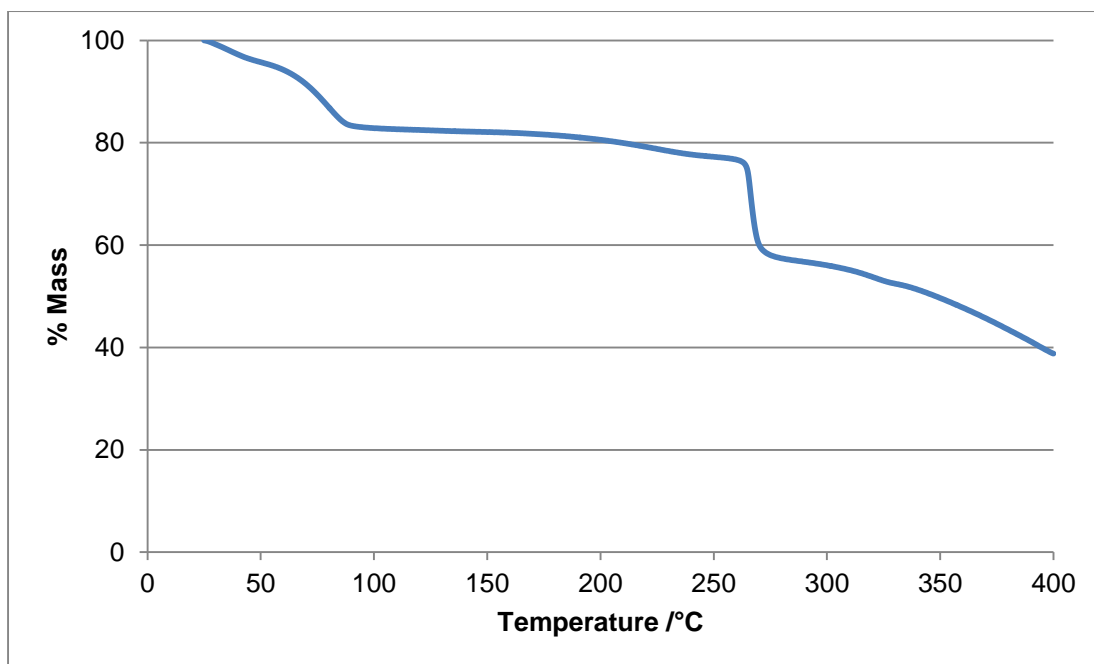


Figure S14: Thermogravimetric analysis trace for Λ -[Cu₄(L-LeuBPSD)₄(OH₂)₂(DMSO)₂] \cdot 2DMSO.

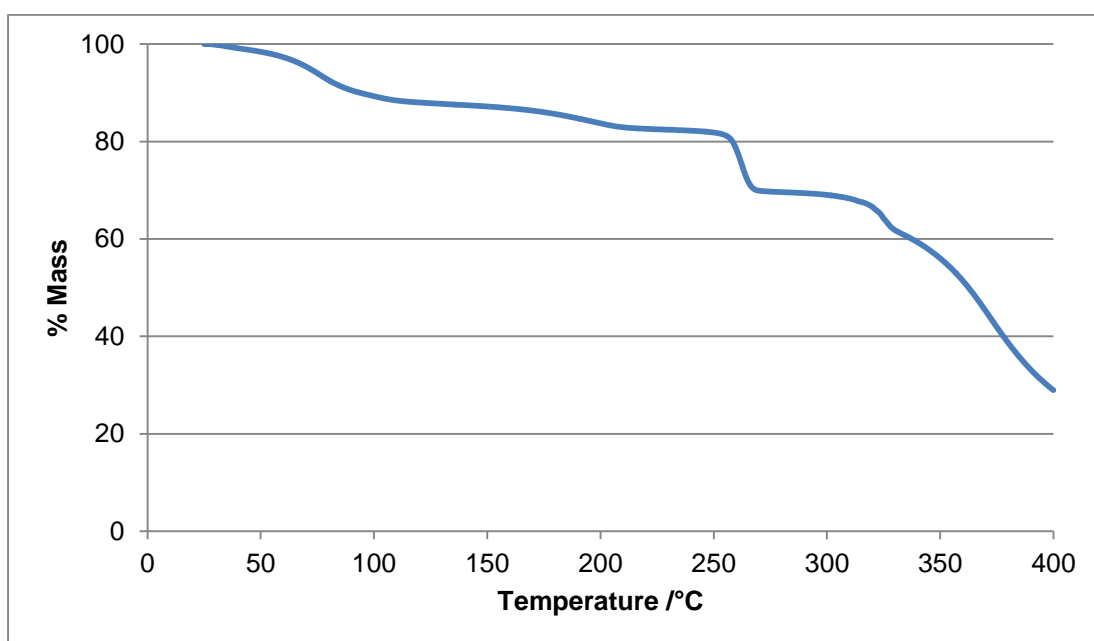


Figure S15: Thermogravimetric analysis trace for Λ -[Cu₄(L-LeuBPSD)₄(MeOH)₂(OH₂)₂]/ Δ -[Cu₄(D-LeuBPSD)₄(MeOH)₂(OH₂)₂] \cdot DMA.

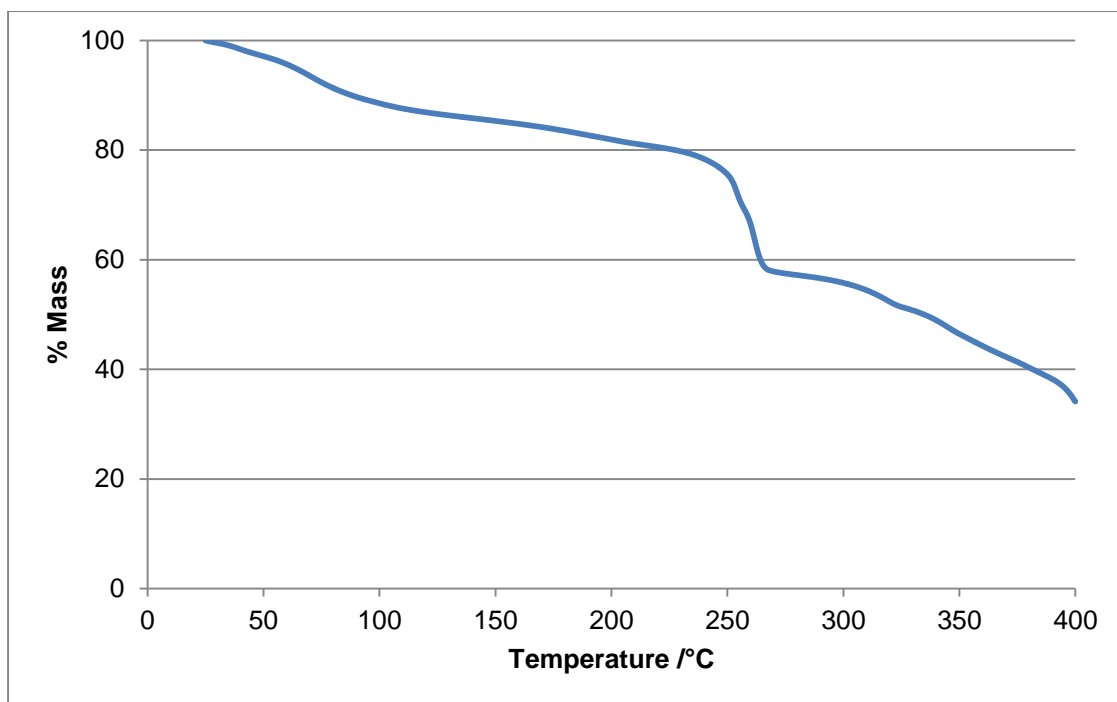


Figure S16: Thermogravimetric analysis trace for $[\text{Cu}_4(\text{DL-H}_2\text{LeuBPSD}_4)(\text{OH}_2)_2(\text{MeOH})_2] \cdot 2\text{DMA}$.

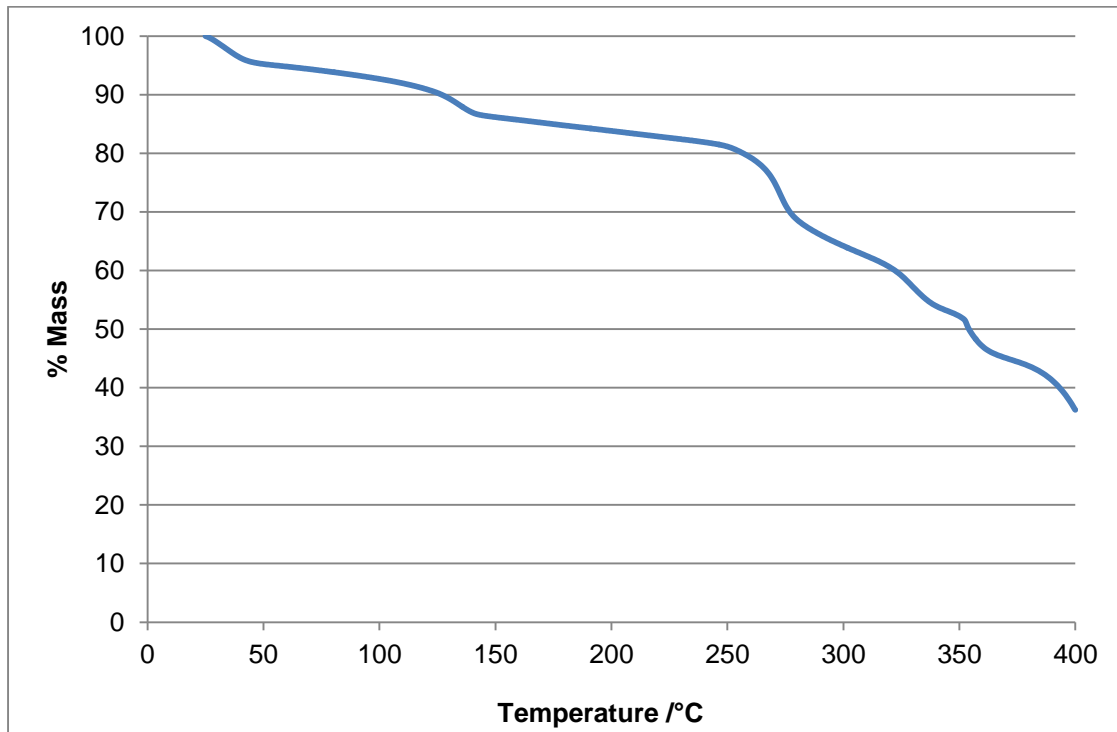


Figure S17: Thermogravimetric analysis trace for $[\text{Cu}_4(\text{GlyBPSD}_4)(\text{MeOH})_3(\text{OH}_2)] \cdot 3.5\text{DMA} \cdot 1.5\text{MeOH}$.

7. Additional Diagrams

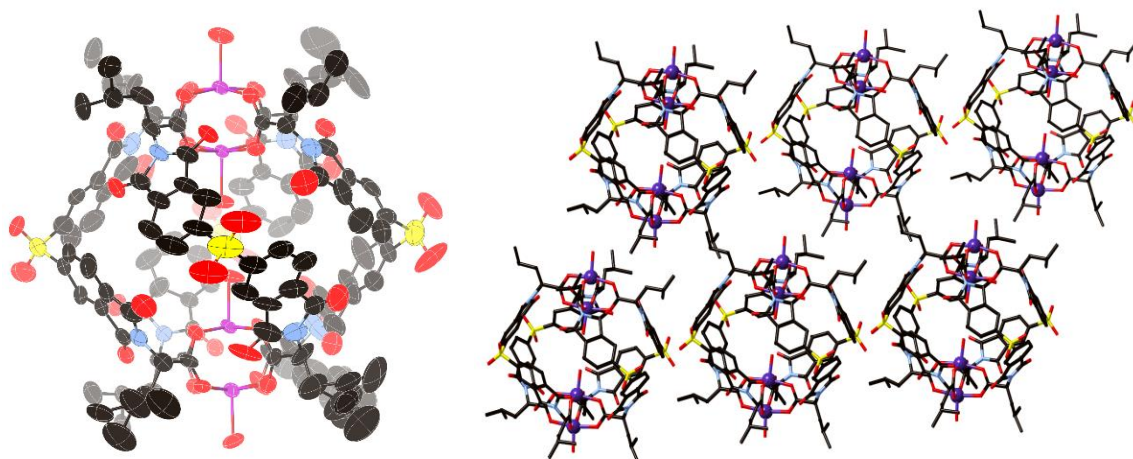


Figure S18: Displacement ellipsoid plot of $[\Lambda\mathbf{1}(\text{OH}_2)_4]$, (left), and packing of $[\Lambda\mathbf{1}(\text{OH}_2)_4]$ cages, (right) in the structure of $\Lambda\text{-}[\mathbf{1}(\text{OH}_2)_4]\cdot 2\text{DMA}$.

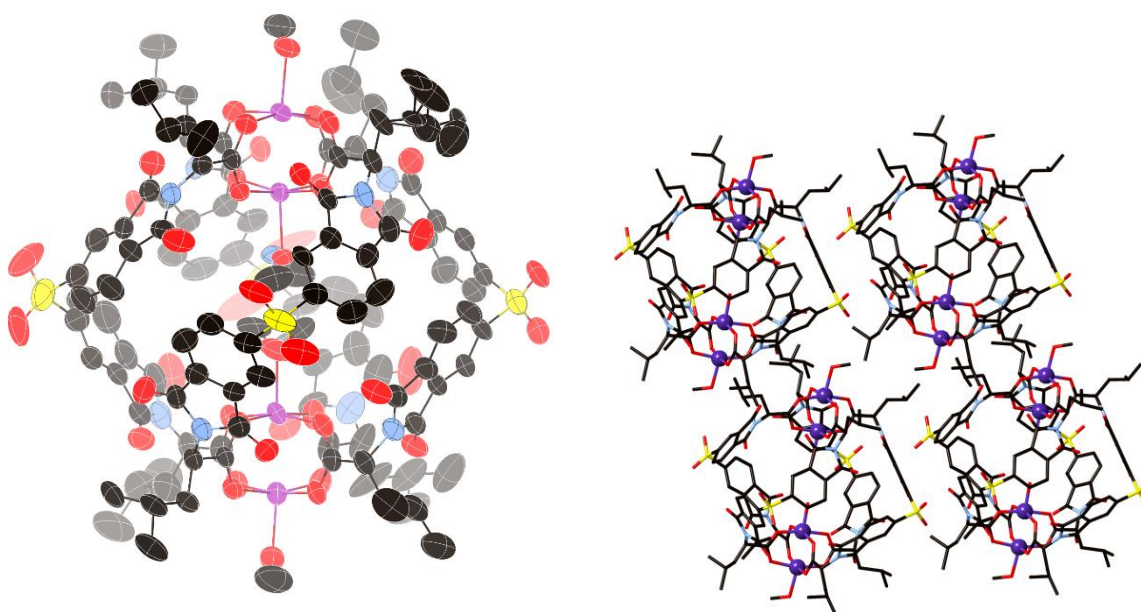


Figure S19: Displacement ellipsoid plot of $[\Delta\mathbf{1}(\text{OH}_2)_2(\text{MeOH})_2]$, (left), and packing of $[\Delta\mathbf{1}(\text{OH}_2)_2(\text{MeOH})_2]$ cages, (right) in the structure of $\Delta\text{-}[\mathbf{1}(\text{OH}_2)(\text{MeOH})_{2.5}(\text{HNMe}_2)_{0.5}]\cdot 4\text{DMA}$.

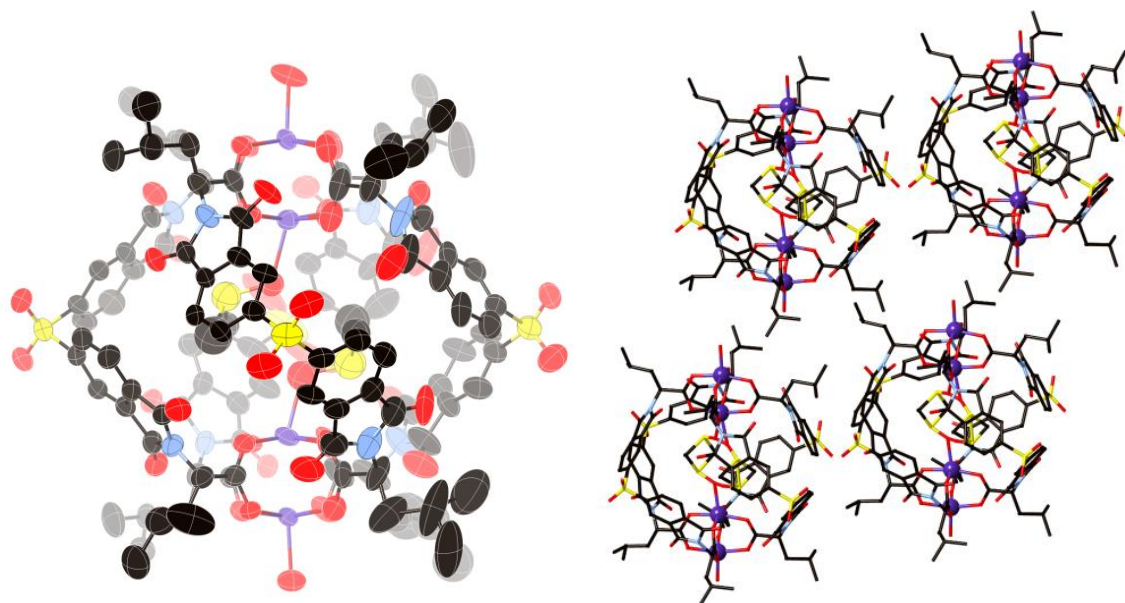


Figure S20: Displacement ellipsoid plot of $[\Lambda 1(\text{OH}_2)_2(\text{DMSO})_2]$, (left), and packing of $[\Lambda 1(\text{OH}_2)_2(\text{DMSO})_2]$ cages (right), in the structure of $[\Lambda 1(\text{OH}_2)_2(\text{DMSO})_2] \cdot 2\text{DMSO}$.

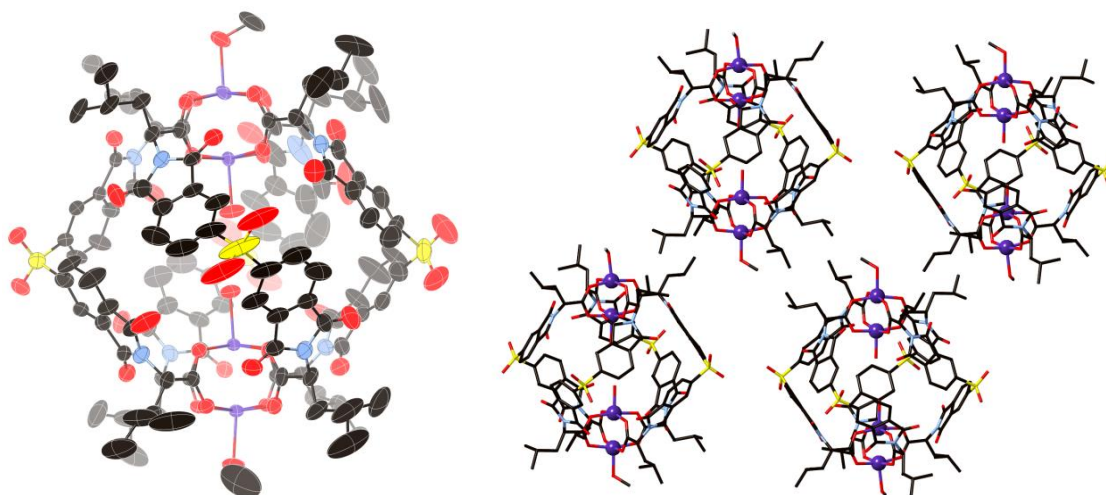


Figure S21: Displacement ellipsoid plot of Λ/Δ - $[1(\text{OH}_2)_2(\text{MeOH})_2]$, (left), and packing diagram of Λ/Δ - $[1(\text{OH}_2)_2(\text{MeOH})_2]$, (right), in the structure of Λ/Δ - $[1(\text{OH}_2)_2(\text{MeOH})_2] \cdot \text{DMA}$.

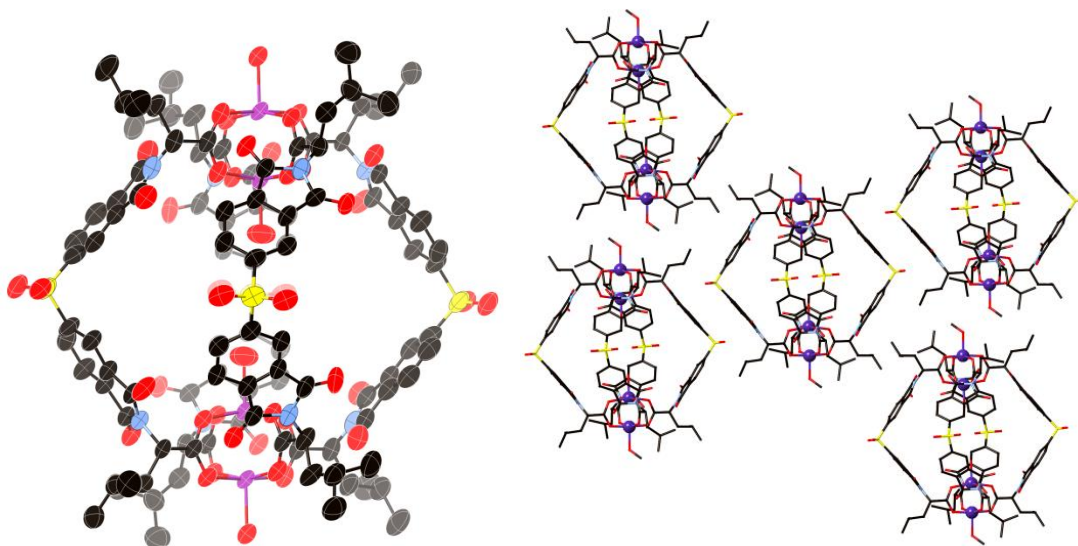


Figure S22: Displacement ellipsoid plot of $[2(\text{OH}_2)_2(\text{MeOH})_2]$, (left) and packing diagram of $[2(\text{OH}_2)_2(\text{MeOH})_2]$, (right) in the structure of $[2(\text{OH}_2)_2(\text{MeOH})_2] \cdot 2.5\text{DMA}$.

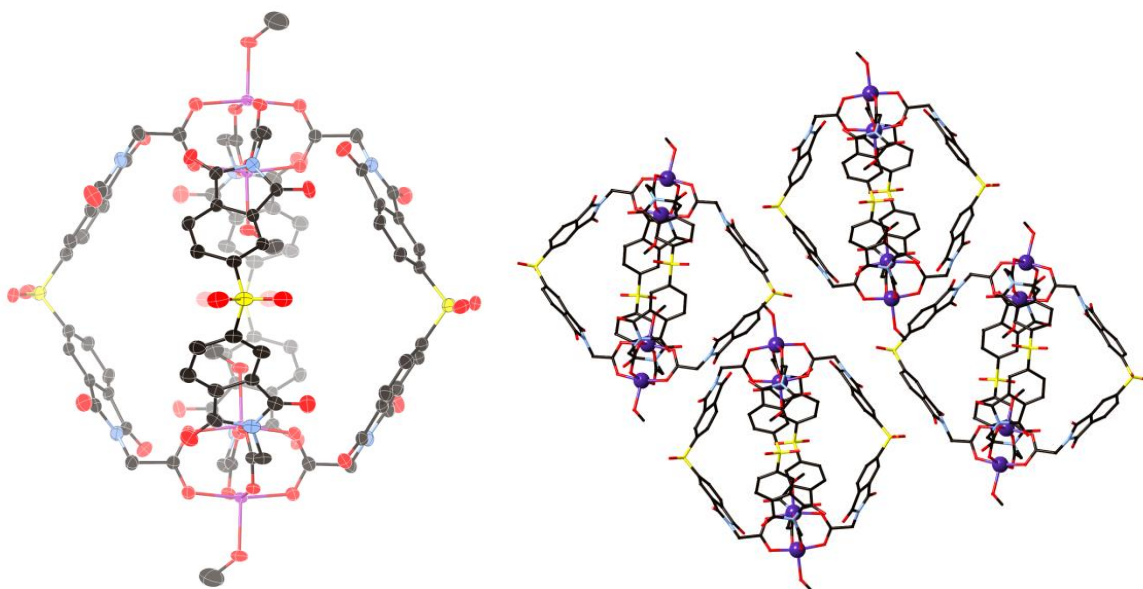


Figure S23: Displacement ellipsoid plot of $[3(\text{MeOH})_3(\text{OH}_2)]$, (left) and packing diagram of $[3(\text{MeOH})_3(\text{OH}_2)]$, (right) in the structure of $[3(\text{MeOH})_3(\text{OH}_2)] \cdot 3.5\text{DMA} \cdot 1.5\text{MeOH}$.

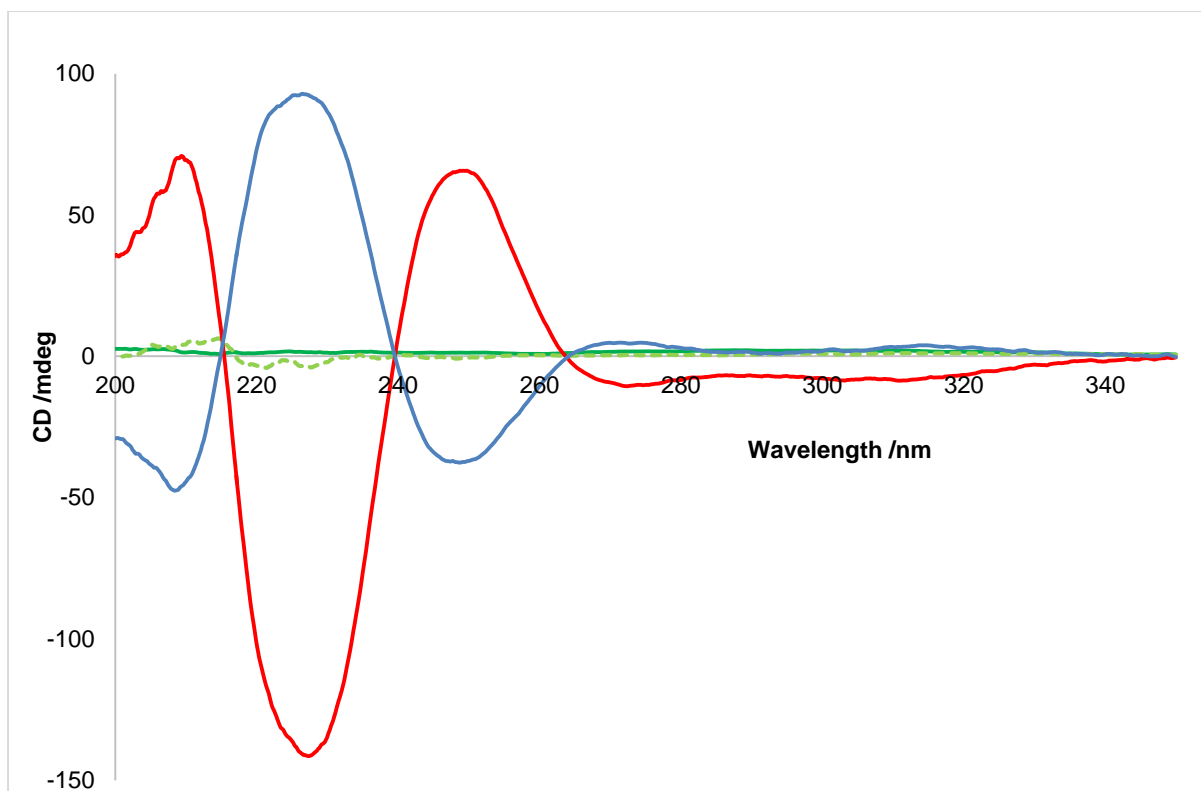


Figure S24: Circular dichroism spectra of cage complexes. Δ -**1** (blue); Λ -**1** (red); dashed, D-H₂LeuBPSD); red (solid,; dashed, L-H₂LeuBPSD); **2** (solid green); DL-H₂LeuDPSD (dashed green).

A. Homochiral Helicates from Enantiopure Ligands

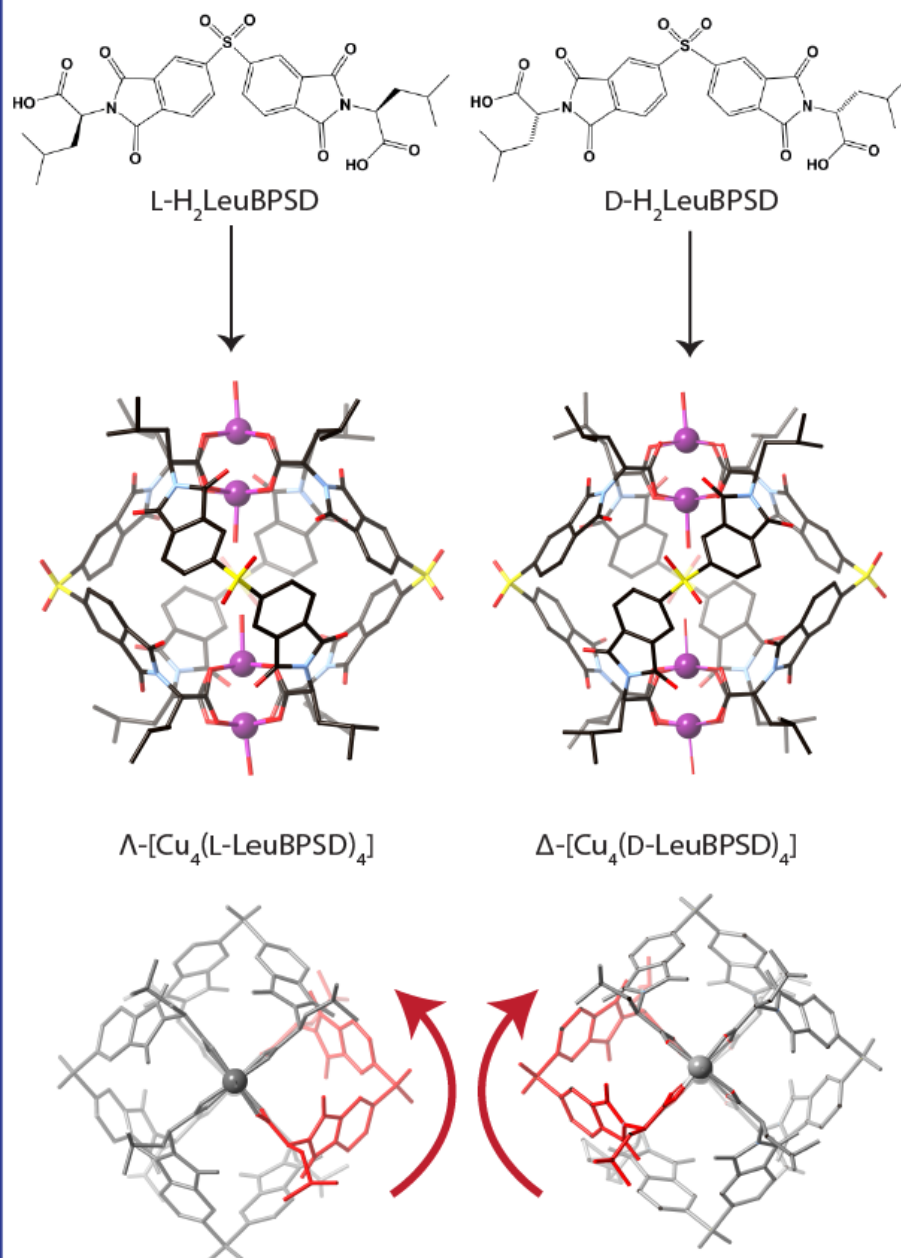


Figure S25: Enlarged version of Fig. 2A.

B. Self-Selecting Homochiral Helicates from Mixture of Enantiopure Ligands

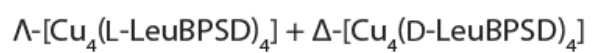
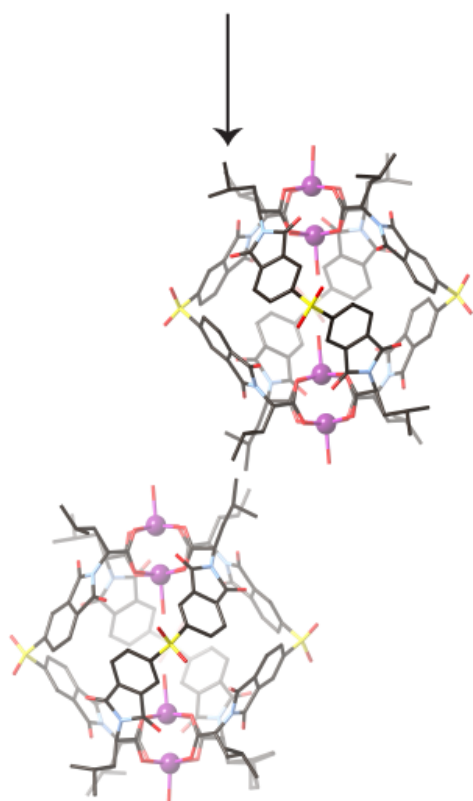
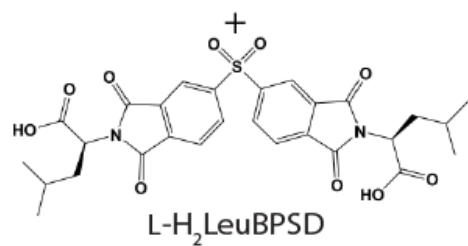
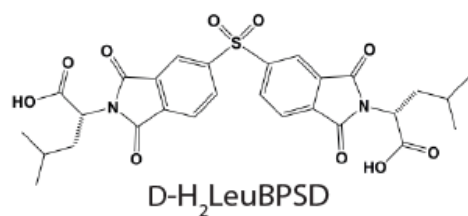


Figure S26: Enlarged version of Fig. 2B.

C. Mesocates from Racemic and Achiral Ligands

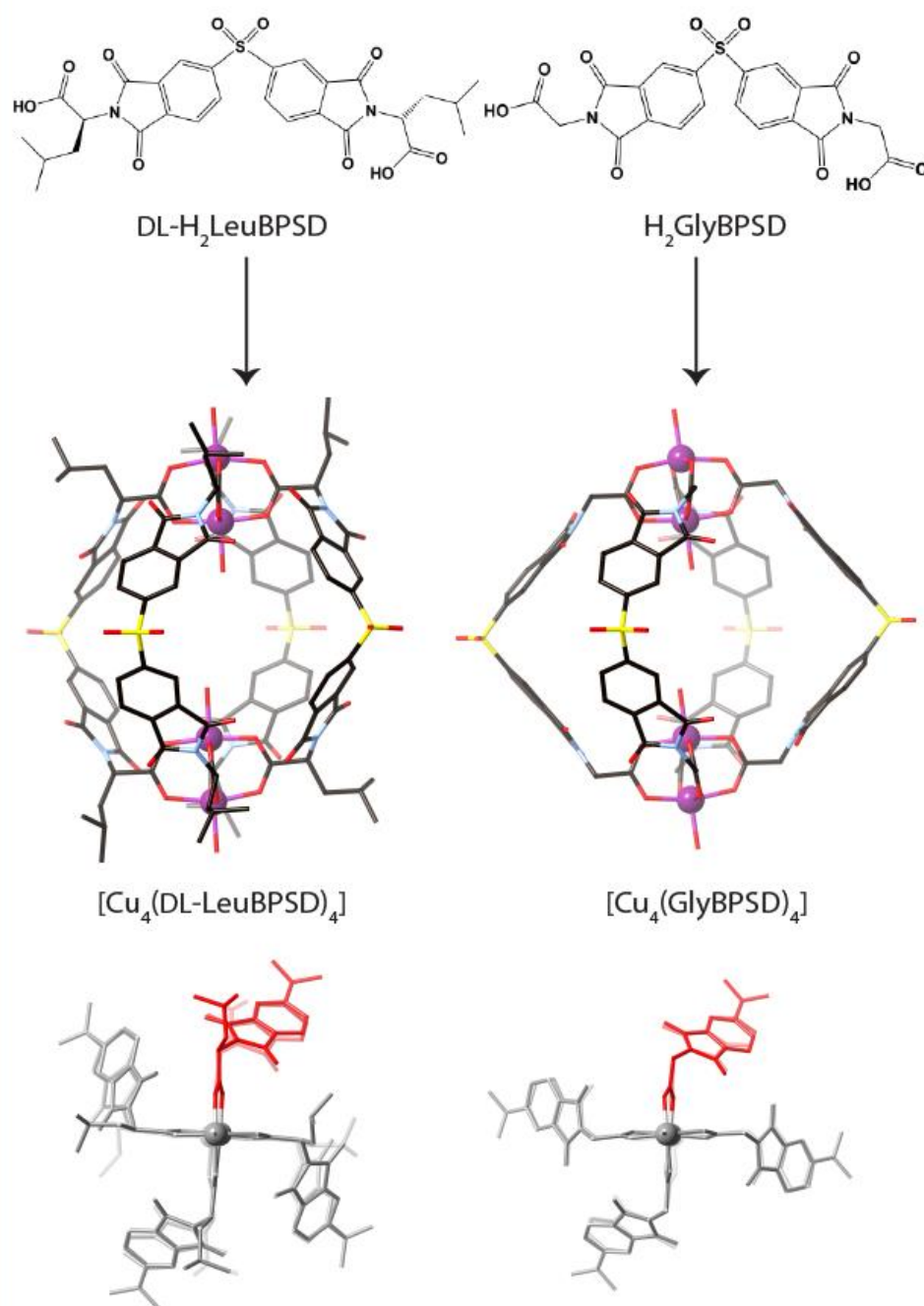


Figure S27: Enlarged version of Fig. 2C.

8. References

- 1 Bruker, SAINT, Bruker AXS Inc., Madison, Wisconsin, USA, 2001.
- 2 T.M. McPhillips, S.E. McPhillips, H.-J. Chiu, A.E. Cohen, A.M. Deacon, P.J. Ellis, E. Garman, A. Gonzalez, N.K. Sauter, R.P. Phizackerly, S.M. Soltis and P. Kuhn, J. *Synchrotron Rad.*, 2002, **9**, 401.
- 3 W.J. Kabsch, *J. Appl. Crystallogr.*, 1993, **26**, 795.
- 4 (a) G.M. Sheldrick, *Acta Crystallogr., Sect. A*, 2008, **64**, 112. (b) SHELXS-2014, G.M. Sheldrick, University of Göttingen, 2014.
- 5 (a) G.M. Sheldrick, *Acta Crystallogr., Sect. A.*, 2015, **71**, 3. (b) SHELXT-2014, G.M. Sheldrick, University of Göttingen, 2014
- 6 (a) G.M. Sheldrick, *Acta Crystallogr., Sect. C*, 2015, **71**, 3. (b) SHELXL-2014, G.M. Sheldrick, University of Göttingen, 2014.
- 7 O.V. Dolomanov, L.J. Bourhis, R.J. Gildea, J.A.K. Howard and H. Puschmann, *J. Appl. Crystallogr.*, 2009, **42**, 339–341.
- 8 (a) A.L. Spek, *Acta Crystallogr., Sect. C*, 2015, **71**, 9. (b) PLATON, A.L. Spek, Utrecht University, 2015.
- 9 S. Parsons, H.D. Flack and T. Wagner, *Acta Cryst., Sect. B*, 2013, **69**, 249.